

# QUANTUM GEOMETRY OF TOPOLOGICAL PHASES OF MATTER

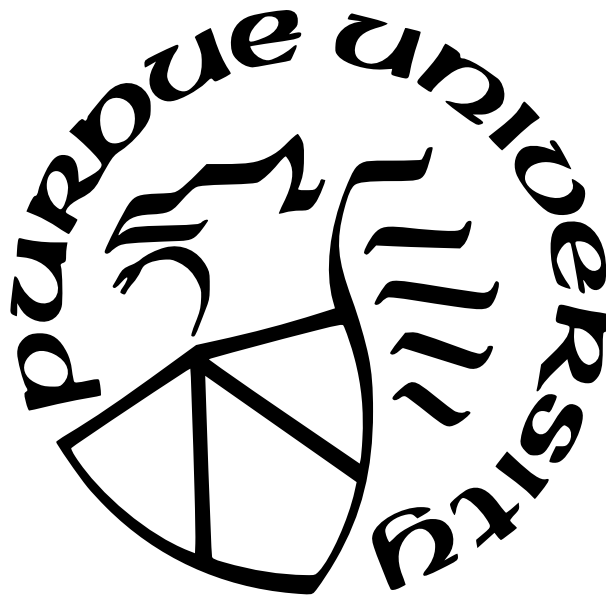
by  
YingKang Chen

A Dissertation

*Submitted to the Faculty of Purdue University*

*In Partial Fulfillment of the Requirements for the degree of*

Doctor of Philosophy



Department of Physics and Astronomy

West Lafayette, Indiana

December 2021

**THE PURDUE UNIVERSITY GRADUATE SCHOOL  
STATEMENT OF COMMITTEE APPROVAL**

**Dr. Rudro R. Biswas, Chair**

Department of Physics and Astronomy

**Dr. Gábor A. Csáthy**

Department of Physics and Astronomy

**Dr. Chris H. Greene**

Department of Physics and Astronomy

**Dr. Srividya Iyer-Biswas**

Department of Physics and Astronomy

**Approved by:**

Dr. Gábor A. Csáthy

## ACKNOWLEDGMENTS

First and foremost, I would like to express my sincere appreciation and gratitude to my advisor, Prof. Rudro R. Biswas, for his continuous encouragement, guidance and especially his patience. I have benefited a lot from his unique insights into physics and sometimes life. Without his help, the work presented in this dissertation would have been impossible. I also want to thank Prof. Srividya Iyer-Biswas, whose advice, enthusiasm and encouragement have been invaluable.

I would also like to thank the rest of my committee members Prof. Gábor A. Csáthy, Prof. Chris H. Greene and also Prof. Srividya Iyer-Biswas, for their time and for reviewing my thesis and sitting through the oral presentation.

I would also like to thank Prof. Sherwin Love, whose Quantum Mechanics and Field Theory courses were legendary. My friends had the good fortune of taking the course, and I heard much from them about how awesome the classes were. Owing to being granted a waiver, I did not have a chance to experience the classes. On the other hand, I benefited greatly from having his all encompassing notes on QM and QFT. Thank you, Sherwin!

Over the years, I have benefited from discussions with my group members. I gratefully acknowledge conversations with GuoDong Jiang, Rishabh Khare and Dewan Woods.

Many thanks to Sandy Formica for reminding me about every deadline and for help with all the paper work. Without Sandy's guidance, I would have been bankrupted by the late fees!

During these years, I am lucky to have many good memories with my friends: WenHao Zhang, Ying Wang, LingYi Dong, JingYi Yang, TaiLung Wu and ZeYong Cai. My sincere gratitude to you all, for digging me out of many holes, for making me feel less isolated.

Last but not least, many thanks to my parents, without whose support and caring I wouldn't have become me.

## CITATIONS TO PREVIOUSLY PUBLISHED WORK

Portions of the Abstract and most of Chapter 2 appear in the publication:

“Gauge-Invariant Variables Reveal the Quantum Geometry of Fractional Quantum Hall States”, Y. Chen and R. R. Biswas, Phys. Rev. B, **102**, 165313 (2020)

Portions of the Abstract and most of Chapter 3 appear in the publication:

“Geometric response of quantum Hall states to electric fields”, Y. Chen, G. Jiang and R. R. Biswas, Phys. Rev. B, **103**, 155303 (2021)

# TABLE OF CONTENTS

LIST OF FIGURES . . . . .	7
ABSTRACT . . . . .	9
1 INTRODUCTION . . . . .	10
1.1 Quantum Hall Effect . . . . .	10
1.2 Topological quantization of Hall conductance . . . . .	13
1.3 Gauge-invariant variables . . . . .	18
1.4 Microscopic origin of the fractional quantum Hall effect . . . . .	20
2 GAUGE-INVARIANT VARIABLES REVEAL THE QUANTUM GEOMETRY OF FRACTIONAL QUANTUM HALL STATES . . . . .	23
2.1 Gauge-invariant variables, again . . . . .	23
2.2 GIV coherent states . . . . .	26
2.3 The Hamiltonian in GIV language . . . . .	28
2.4 GIV Schrödinger equation . . . . .	29
2.5 Example: Laughlin state . . . . .	33
2.6 Summary . . . . .	34
3 GEOMETRIC RESPONSE OF QUANTUM HALL STATES TO ELECTRIC FIELDS	36
3.1 Wavefunctions in the GIV formalism . . . . .	37
3.2 Motion in a non-uniform electric field . . . . .	41
3.2.1 Landau-level projection . . . . .	42
3.2.2 Beyond Landau-level projection - an effective Hamiltonian . . . . .	44
3.3 Local observables in a non-uniform electric field . . . . .	50
3.3.1 Local current density - analytical approach . . . . .	51
3.3.2 Local charge density - analytical approach . . . . .	54
3.3.3 Numerical checks of analytical calculations . . . . .	57
3.4 Summary . . . . .	60

REFERENCES . . . . .	62
----------------------	----

## LIST OF FIGURES

1.1	Setup for measuring the Hall conductivity, $\sigma_H = V_H/I$ . . . . .	10
1.2	Particle on a ring with magnetic flux, $\Phi$ , piercing the ring. . . . .	13
1.3	Laughlin's setup for showing the topological quantization of the Hall conductance. . . . .	14
2.1	Comparing kinematic formulations of planar quantum mechanics in the presence of a magnetic flux, $\mathbf{B}$ , using (a) conventional position and linear momentum, vs. (b) gauge-invariant variables (GIVs), namely, the kinetic momenta, $\boldsymbol{\pi}$ , and the guiding center coordinates, $\mathbf{R}$ . In (b), adding interactions is the only modification to the simple 'free' picture necessary, for describing strongly correlated fractional quantum Hall phases. In contrast, in (a), first the magnetic field needs to be incorporated and then interactions are added in. . . . .	24
3.1	A geometric summary of how a non-uniform electric field, $\mathbf{E}$ , deforms a cyclotron orbit. The changes can be expressed in terms of a vector field, $\boldsymbol{\Delta}(\mathbf{R})$ (Eq. (3.25b)), and a shearing field, $\Lambda(\mathbf{R})$ (Eq. (3.28b)). The new orbit is shifted by amount $\boldsymbol{\delta}(\mathbf{R}) = \hat{\mathbf{z}} \times \boldsymbol{\Delta}(\mathbf{R})$ with respect to the original center, $\mathbf{R}$ , and acquires a drift velocity, $\mathbf{v}_d = \boldsymbol{\Delta}(\mathbf{R})$ . The orbit is also sheared into an ellipse with aspect ratio $\lambda^2$ ; see Eq. (3.34) and accompanying text for details. The guiding center coordinate, $\mathbf{R}$ , labels the field-free orbit center while the kinetic momentum, $\boldsymbol{\pi}$ , gives the velocity of the electron (Eq. (2.1)). . . . .	37
3.2	Equipotentials in a typical disordered material. The red dots show random potential centers used to simulate this example. These equipotentials are localized and closed in the bulk while those at the boundary run along the entire perimeter of the material. Since guiding center eigenstates run along these equipotentials (see accompanying text), those the bulk are localized. The extended guiding center states along the edge are the well-known edge states, which account for the quantized Hall conductance of a filled Landau level. . . . .	44
3.3	The variation of cyclotron orbit energy with orbit location, $\bar{x}$ . The Landau levels are modeled by the lowest bands in a Hofstadter model on a square lattice. The nonuniform electric field is generated by a sinusoidal background potential, which is small compared to the inter-Landau-level energy gap, so that the system is in the linear response regime. The brown circles correspond to the cyclotron energies obtained via numerical diagonalization. The dashed green curve is the sum of the Landau level energy and the local potential energy, which is the correct energy when the electric field is uniform. The thick blue curve corresponds to Eqs. (3.33) and (3.55), correct up to the second order in the derivatives of the electric field. For these plots, $V_0/\epsilon_c = 0.05$ , $k\ell = 0.65$ . . . . .	57

- 3.4 The spatial variation of local current density in a nonuniform (sinusoidal) electric field. The Landau levels are modeled by the lowest bands in a Hofstadter model on a square lattice. The nonuniform electric field is generated by a sinusoidal background potential, which is small compared to the inter-Landau-level energy gap so that the system is in the linear response regime. The brown circles correspond to the local current density values obtained via numerical diagonalization. The dashed green curve is the quantized local Hall response, which is correct when the electric field is uniform. The thick blue curve corresponds to Eqs. (3.47) and (3.56), correct up to the second order in the derivatives of the electric field. For these plots,  $V_0/\epsilon_c = 0.05$ ,  $k\ell = 0.32$ . . . . . 58
- 3.5 The spatial variation of local fractional charge density modulation in a nonuniform (sinusoidal) electric field. The Landau levels are modeled by the lowest bands in a Hofstadter model on a square lattice. The nonuniform electric field is generated by a sinusoidal background potential, which is small compared to the inter-Landau-level energy gap so that the system is in the linear response regime. The brown circles correspond to the local charge density values obtained via numerical diagonalization. The dashed green curve is the response obtained correct to the second derivative in the electric field, Eq. (3.50), corresponding to the nonuniform polarization induced by cyclotron orbit shifts. The thick blue curve corresponds to Eqs. (3.51) and (3.57), correct to the third order in the derivatives of the electric field. For these plots,  $V_0/\epsilon_c = 0.05$ ,  $k\ell = 0.49$ . . . . . 59



# ABSTRACT

Quantum Hall states are prototypical topological states of matter whose Hall conductance is topologically quantized to an integer or rational fraction multiple of the fundamental conductance quantum. A significant consequence of this quantization is that the Hall conductance value can be made independent of variations from device to device, within acceptable limits. Such topologically quantized properties are thus highly desirable for metrology or industrial purposes. Formulating a microscopic picture of fractional quantum Hall states and the characterization of all topological responses of quantum Hall states are frontier areas of condensed matter research, with far reaching technological consequences such as realizing anyonic topological quantum computation. In this dissertation, I will present my research on these topics.

We will begin with a brief review of integer and fractional quantum Hall effects, a recounting of topological reasons underlying the universal quantization of the Hall conductance in insulators and a presentation of basic quantum mechanical microscopic descriptions of these states.

In Chapter 2, we introduce the framework of gauge-invariant variables to describe fractional quantum Hall states, and prove that the wave function can always be represented by a unique holomorphic multivariable complex function. As a special case, within the lowest Landau level, this function reproduces the well-known holomorphic representation of wave functions in the symmetric gauge. Using this framework, we derive an analytic guiding center Schrödinger's equation governing FQH states, establishing a new avenue for deriving the properties of FQH states from first principles.

In Chapter 3, again using the language of gauge-invariant variables to analyze the quantum mechanics of quantum Hall states, we provide tangible connections between the response of quantum Hall fluids to nonuniform electric fields and the characteristic geometry of electronic motion in the presence of magnetic and electric fields. The geometric picture we provide motivates the following ansatz: nonuniform electric fields mimic the presence of spatial curvature. Consequently, the gravitational coupling constant also appears in the charge response to nonuniform electric fields.

# 1. INTRODUCTION

## 1.1 Quantum Hall Effect

The discovery of the quantum Hall effects[1], [2], four decades ago, started a scientific revolution whose effects remain undiminished in contemporary condensed matter physics research. These effects and the states of matter they reveal have matured into the research area of topological quantum materials and serve as paradigms for discovering new topological phenomena. This dissertation is devoted to investigations of new techniques that reveal new properties of the quantum Hall (QH) states, i.e., electronic states which display the quantum Hall effect.

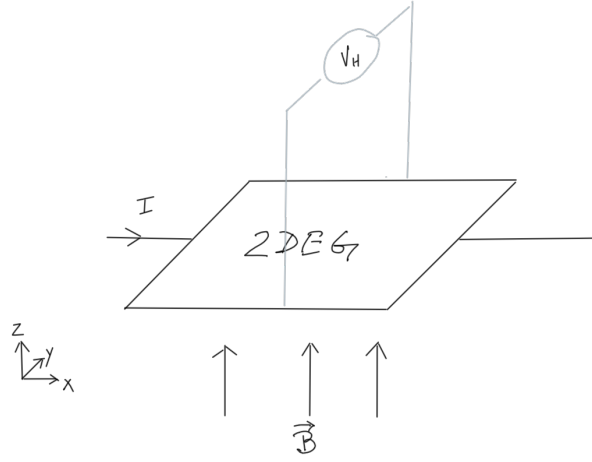


**Figure 1.1.** Setup for measuring the Hall conductivity,  $\sigma_H = V_H/I$ .

First, a brief introduction to the quantum Hall effect (QHE), which is the observation of quantized Hall conductance in two dimensional electronic gases (2DEGs). The measurement setup for observing QHE is as shown in Figure 1.1. A 2DEG (usually a quantum well inside a semiconductor heterostructure) is placed in a perpendicular uniform magnetic field and a current,  $I$ , passed through it, say in the  $x$ -direction. A non-Ohmic voltage drop appears across the  $y$ -direction: this is the Hall voltage,  $V_H$ . The Hall conductance is the ratio:

$$\sigma_H = \frac{I}{V_H}. \quad (1.1)$$

In a classical mechanical model of charged particles carrying current, with individual charges  $e^*$  and areal density  $n_{e^*}$ , the existence of the Hall voltage is necessary to balance the Lorentz force that would bend the current otherwise, yielding the classical expression for the Hall conductivity:

$$\sigma_H^{(c)} = \frac{e^* n_{e^*}}{B}. \quad (1.2)$$

Such inverse variation with the magnetic field is indeed observed in usual experiments (small magnetic fields, disordered materials, temperatures not too low). Thus, measuring the Hall conductivity vs the inverse magnetic field yields the charge density of current carriers in the material, a very useful characteristic of a material. In seminal experiments from 1980 [1] and 1982 [2], working with high magnetic fields and very clean 2DEGs, it was discovered that the classical formula breaks down and quantized plateaus emerge as a function of the magnetic field. At these plateaus, the Hall conductance is quantized at integer or certain rational fraction multiples of the conductance quantum,  $e^2/h$ , which is a combination of material-agnostic fundamental constants (electric charge and Planck's constant). Simultaneously, the Ohmic conductance becomes zero, indicating the existence of a bulk energy gap for charge carriers that precludes dissipation. This remarkable phenomenon is known as the Quantum Hall Effect.

When the Hall conductance is an integer multiple of  $e^2/h$ , the phenomenon is known as the Integer Quantum Hall Effect (IQHE) and the 2DEG is said to be in an Integer Quantum Hall (IQH) state. Such electronic states can be understood using a non-interacting yet quantized picture of electrons moving in a magnetic field, which leads to the formation of macroscopically degenerate Landau levels with spectral gaps separating successive levels. An integer QH state can be modeled as a sequence of completely filled Landau levels, with a Hall conductivity of  $e^2/h$  per filled Landau level.

When the Hall conductance is a non-integer rational fraction multiple of  $e^2/h$ , the phenomenon is known as the Fractional Quantum Hall Effect (FQHE) and the 2DEG is said to be in a Fractional Quantum Hall (FQH) state. Understanding such states is more difficult, since it requires incorporation of strong electronic correlations. The breakthrough in

understanding the origins of FQHE was provided by Laughlin in a seminal paper from 1983 [3], wherein he constructed a sequence of strongly correlated many-electron wave functions that characterize energetically gapped incompressible quantum ground states with electronic charge densities that are rational fraction multiples of the Landau level charge density. A 2DEG in one of such Laughlin states, if it is a gapped ground state, would exhibit FQHE with Hall conductivity  $e^2/(ph)$ , where  $p$  is an odd integer. Following this idea, many such model wave functions have been conjured for describing other FQH states. While it is widely believed that such wave functions are representative of FQH states observed in real experiments, direct calculation of FQH state properties from first principles, necessary for describing and predicting experimental details, is still a difficult task [4].

A subtle point: in two dimensions, such as in the 2DEGs mentioned above, the conductance and conductivity have the same units. Naïvely, the conductivity is fixed for a given material but the conductance of a device is related to the conductivity by a device-dependent factor. Remarkably then, it is the Hall conductance of a real-world device with disorder that is quantized (fixed) in a quantum Hall experiment; the Hall conductance is found to be equal to the bulk Hall conductivity of the corresponding clean quantum Hall state. We will touch upon the topic of disorder in the last chapter when we deduce the response of a clean quantum Hall state to weak non-uniform electric fields.

The plan for the rest of this dissertation is as follows. In the following sections, we will introduce universal reasoning showing why the Hall conductance is quantized, followed by brief discussions of the language of gauge-invariant variables, a recurring theme in this dissertation, and fractional quantum Hall states. In Chapter 2, we will introduce a new framework of coherent states based on gauge-invariant variables, which will allow framing the first principles calculation of FQH physics on an analytic footing. Finally, in Chapter 3, we will use gauge-invariant variables, combined with the Wigner pseudoprobability function, to derive a novel aspect of the response of QH states to non-uniform electric fields: this response incorporates the quantized gravitational coupling coefficient characterizing local charge response of QH states to real space curvature!

## 1.2 Topological quantization of Hall conductance

We will now present Laughlin's argument [5], [6] for the quantization of Hall conductance, where the fundamental physics principles of gauge invariance and charge quantization play central roles.

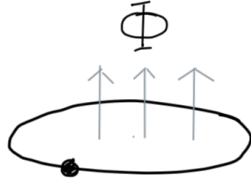


**Figure 1.2.** Particle on a ring with magnetic flux,  $\Phi$ , piercing the ring.

A prototypical example that exhibits the topological thinking underlying Laughlin's thought experiment is that of a particle moving in a circle of radius  $R$ , in the presence a variable magnetic flux,  $\Phi$ , piecing through the center of the circle (see Figure 1.2). Parametrizing the particle coordinate by the angle  $\phi$ , the Hamiltonian is:

$$H = \frac{1}{2mR^2} \left( p_\phi + \frac{e\Phi}{2\pi} \right)^2 = \frac{1}{2mR^2} \left( -i\frac{\partial}{\partial\phi} + \frac{\Phi}{\Phi_0} \right)^2,$$

where  $\Phi_0 = 2\pi\hbar/e$  is the flux quantum. The energy eigenvalues are

$$E_{n,\Phi} = \frac{1}{2mR^2} (n + \Phi/\Phi_0)^2,$$

while the corresponding energy eigenstates are

$$\psi_{n,\Phi} = \frac{1}{\sqrt{2\pi}} e^{in\phi}, \quad n \in \mathbb{Z}.$$

Suppose now that the particle is in a specific energy eigenstate and  $\Phi = 0$ . Let us now slowly increase the flux by one flux quantum ( $\Phi_0$ ), on timescales much larger than the one corresponding to the energy gaps between states. We can then use the adiabatic theorem, which states that the particle continues to remain in the instantaneous quantum state. At the end of the above process the final inserted flux,  $\Phi_0$ , can be removed by a gauge

transformation. Thus, the final energy spectrum is identical to the spectrum when the flux was absent at the beginning of the process: the set of initial energies at zero flux,  $\{\dots, E_{-1,0}, E_{0,0}, E_{1,0}, \dots\}$ , is the same as the energies at unit flux  $\{\dots, E_{-1,1}, E_{0,1}, E_{1,1}, \dots\}$ , where the flux is measured in units of the flux quantum. Does this mean that the particle returns to its original state? No! Following the evolution of each energy eigenstate with  $\Phi$ , we can also see that each eigenstate shifts to the next eigenstate in the sequence:  $E_{n-1,1} = E_{\pm n,0} = E_{-n-1,1}$ ,  $\psi_{n-1,0} \rightarrow \psi_{n-1,1}$ ,  $\psi_{-n-1,0} \rightarrow \psi_{-n-1,1}$ . This phenomenon is called *spectral flow*. The particle is thus ‘pumped’ into the next energy eigenstate, a topologically nontrivial outcome.

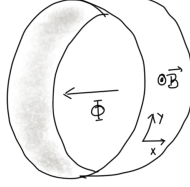


**Figure 1.3.** Laughlin’s setup for showing the topological quantization of the Hall conductance.

We can now explicitly present Laughlin’s argument for Hall conductance quantization in integer quantum Hall states. Instead of a ring threaded by a flux, we use a cylindrical surface threaded by a flux  $\Phi$  (Figure 1.3). There is a radial uniform magnetic field  $B$  penetrating the cylindrical surface. The radius of the cylinder is  $R$ , the width is  $L_x$ . The  $x$  coordinate is chosen to be along the longitudinal direction of the cylinder (opposite  $\Phi$ ),  $y$  coordinate is along the circumference and we choose the Landau gauge for expressing the vector potential,  $\mathbf{A} = (Bx + \Phi/(2\pi R))\hat{\mathbf{y}}$ . The Hamiltonian is:

$$\begin{aligned} H &= \frac{1}{2m} \left( p_x^2 + \left( p_y + eBx + \frac{e\Phi}{2\pi R} \right)^2 \right) \\ &= \frac{1}{2m} \left( p_x^2 + (eB)^2 \left( x + \frac{p_\phi}{eBR} + \frac{\Phi}{\Phi_0 \cdot eBR} \right)^2 \right). \end{aligned}$$

Bulk eigenstates of this Hamiltonian are given by Gaussian-shaped strips running parallel to the  $y$  direction:

$$\psi_{n,m} \propto e^{iny/R} \varphi_m \left( \frac{x}{\ell} + \frac{n + \Phi/\Phi_0}{R/\ell} \right),$$

where  $\varphi_m$  is the  $m^{\text{th}}$  eigenstate of the quantum simple harmonic oscillator and  $\ell = \sqrt{\frac{\hbar}{eB}}$  is called magnetic length. We have assumed that  $L_x \gg \ell$  for simplicity. The corresponding energies are:

$$E_{n,m} = \frac{1}{2} \omega_c \left( m + \frac{1}{2} \right),$$

which are independent of  $n$  and so are degenerate.  $\omega_c = \sqrt{\frac{eB}{m}}$  is called the cyclotron frequency. These degenerate energy levels, separated by the cyclotron energy  $\hbar\omega_c$ , are the famed Landau levels.

In  $x$ -direction,  $\psi_{n,m}$  is centered at  $-\frac{\ell^2}{R}(n + \Phi/\Phi_0)$ . Thus, increasing  $\Phi$  results in the wave function moving to smaller  $x$ . Specifically, increasing  $\Phi$  by  $\Phi_0$  makes each state move to its neighbor's spot in the lower  $x$  direction. This is the nature of *spectral flow* in this system.

For each Landau level  $m$ , there are at most  $N$  strips, where  $N$  is determined by the condition that the wavefunction center should be located within the range  $(0, L_x)$ . Thus,  $N \cdot \ell^2/R = L_x$ , and so  $N = RL_x/\ell^2 = (2\pi RL_x)B/\Phi_0$ . In other words, the total degeneracy of a Landau level is given by the number of flux quanta piercing the 2DEG and is thus *extensive* (proportional to area)! Now, consider a completely filled Landau level with  $N$  electrons (ignoring spin). This is a gapped state and does not exhibit Ohmic transport at low temperatures. Suppose we now increase the flux  $\Phi$  slowly and steadily from  $\Phi = 0$  to  $\Phi = \Phi_0$ . By the adiabatic theorem, because of the presence of the energy gap to excitations, the electrons will continue to remain in the instantaneous ground state determined by the spectral flow described above. Since all electronic states have to move one slot over in the negative  $x$  direction, a total charge of  $e$  (positive) will effectively move across the cylinder in the  $x$  direction. Since the EMF generated by this adiabatic change of magnetic flux in the

$y$ -loop is  $V_H = (\partial\Phi/\partial t) = (\Phi_0/T)$  (where  $T$  is the time for adiabatic change), we see that the total current in the  $x$ -direction is:

$$I_x = \frac{e}{T} = (e\Phi_0)V_H \equiv \sigma_H V_H. \quad (1.3)$$

Thus the Hall conductance of a filled Landau level, also equivalent to the Hall conductivity because of uniformity of the filled Landau level charge density, is simply  $\sigma_H = e\Phi_0 = e^2/h$ , the universal conductance quantum.

If we consider a ground state with  $n$  fully filled Landau levels, then  $n$  electrons will be transferred per flux quantum increase in  $\Phi$ , therefore the Hall conductance is  $\sigma_H = ne^2/h$ . Such a quantum state thus provides a good model for the appropriate IQH state.

The key ingredient in above arguments is that the effect of the inserted flux  $\Phi$  on a gapped quantum state (i.e., an insulator) is periodic in integer multiples of flux quantum  $\Phi_0$ , a consequence of the fundamental physical principle of gauge invariance. Thus, at the end of  $\Phi_0$  change in  $\Phi$ , due to the principle of charge quantization, an integer number of electronic charges need to flow across the 2DEG in the direction perpendicular to the electric field, yielding a Hall conductance that is an integer multiple of  $e^2/h$ . Thus the quantization of the Hall conductance is a universal topological consequence of spectral flow in insulators, relying only on fundamental physics principles.

If strong correlations yield multiple degenerate ground states of the 2DEG, the above argument needs to be modified somewhat [7]. Now, changing  $\Phi$  by  $\Phi_0$  brings the Hamiltonian back to its original form, but the system may return to a different ground state than the one it started from! Repeating this process  $q$  times, the system will finally come back to the original ground state, by which time an integer  $p$  number of  $e$  charges have to be transported across the system. The system thus has a Hall conductivity of  $(p/q)$  conductance quanta, i.e., it exhibits the FQHE. Thus, we see that both types of quantization of Hall conductance, integer or fractional, are consequences of universal physics principles.

We will now close with a formal topological description of the integer quantum Hall effect, following Niu's work [7]. We have seen above that for a gapped insulator with a unique ground state parametrized by the flux  $\Phi$ , the parameter space is equivalent to a



circle:  $\Phi/\Phi_0 \in [0, 1)$ . Instead of a cylindrical surface, consider placing the 2DEG on a torus, with fluxes threaded through the two holes of the torus. (These fluxes can alternately be replaced by phase twists across the two periodic directions of the torus.) Suppose the two dimensions of the torus are given by  $L_x$  and  $L_y$ , then the vector potential in the Landau gauge is

$$\begin{aligned} A_x &= \frac{\Phi_x}{L_x}, \\ A_y &= \frac{\Phi_y}{L_y} + Bx. \end{aligned}$$

The two components of the current operator are given by  $J_i = -\frac{1}{L_i} \partial H / \partial \Phi_i$ . Denote the many-body states, arranged in order of increasing  $n$ , by  $|\psi_n\rangle$  (equivalently,  $|n\rangle$ ) and assume that the ground state,  $|\psi_0\rangle$ , is not degenerate. The Kubo formula for Hall conductance yields:

$$\sigma_{xy} = i\hbar \sum_{n \neq 0} \frac{\langle 0 | J_y | n \rangle \langle n | J_x | 0 \rangle - \langle 0 | J_x | n \rangle \langle n | J_y | 0 \rangle}{(E_n - E_0)^2}.$$

Using the formula  $\langle m | \partial_{\Phi_i} | n \rangle = \frac{1}{E_n - E_m} \langle m | (\partial_{\Phi_i} H) | n \rangle$ , we can simplify:

$$\begin{aligned} \sigma_{xy} &= i\hbar \sum_{n \neq 0} \langle \partial_{\Phi_y} \psi_0 | \psi_n \rangle \langle \psi_n | \partial_{\Phi_x} \psi_0 \rangle - \langle \partial_{\Phi_x} \psi_0 | \psi_n \rangle \langle \psi_n | \partial_{\Phi_y} \psi_0 \rangle \\ &= \frac{e^2}{h} \cdot \frac{i}{2\pi} \left( \partial_{\theta_y} \langle \psi_0 | \partial_{\theta_x} \psi_0 \rangle - \partial_{\theta_x} \langle \psi_0 | \partial_{\theta_y} \psi_0 \rangle \right), \end{aligned}$$

where  $\theta_i = \frac{\Phi_i}{\Phi_0}$ . Again, by gauge invariance, nothing changes if the changes of  $\Phi_i$  are integer multiples of  $\Phi_0$ . Thus,  $\theta_i$  can be viewed as coordinate of a torus  $\mathbb{T}^2$ . Then the states  $|\psi_n\rangle$  are sections on the torus  $\mathbb{T}^2$ . The expression inside the parenthesis is the Berry curvature  $F_{xy}$ , therefore the conductance can be written in the form

$$\sigma_{xy} = \frac{e^2}{h} \cdot \frac{i}{2\pi} F_{xy} = \frac{e^2}{2\pi\hbar} \cdot c_1(F),$$

where  $c_1(F) = \frac{i}{2\pi} F_{xy}$  is the 1<sup>st</sup> Chern form. Since the process of turning on an electric field is tantamount to the phases  $\theta_i$  changing in time, the observed Hall conductance is an average of the Kubo formula over the entire  $\theta$ -torus:

$$\sigma_{xy} = \frac{e^2}{h} \iint_{\mathbb{T}^2} c_1(F) = \frac{e^2}{h} C, \quad (1.4)$$

where  $C$  the 1<sup>st</sup> Chern number, an integer-valued topological index (a generalized winding number) that characterizes the variation of the many-body ground state over the torus of boundary conditions/fluxes. This formula thus explicitly and formally connects the Hall conductance with the topology of the  $U(1)$  vector bundle, the ground state many-body wave function defined over the torus  $\mathbb{T}^2$ .

### 1.3 Gauge-invariant variables

Consider a non-interacting 2DEG moving under the influence of an uniform magnetic field perpendicular to the plain:

$$H = \frac{1}{2m} (\mathbf{p} + e\mathbf{A})^2 = \frac{1}{2m} \boldsymbol{\pi}^2, \quad (1.5)$$

where  $\mathbf{A}$  gives the magnetic field  $\mathbf{B} = \nabla \times \mathbf{A} = B\hat{\mathbf{z}}$ . Contrary to the conventional approach of choosing a gauge as described in the previous section, we will not assume any particular gauge now.  $\boldsymbol{\pi}$  is called the mechanical or kinetic momentum. Contrary to naive expectation, the two components of  $\boldsymbol{\pi}$  do not commute:

$$\begin{aligned} [\pi_i, \pi_j] &= [p_i + eA_i, p_j + eA_j] = e\epsilon_{ij}[p_i, A_j] = -ie\epsilon_{ij}\partial_i A_j \\ &= -ie\epsilon_{ij}B, \end{aligned} \quad (1.6)$$

which reminds us the commutation relation of the canonical coordinate and canonical momentum. Here,  $\epsilon$  is Levi-Civita tensor in two dimensions. Thus, the Hamiltonian  $H$  can be thought of as an harmonic oscillator (SHO) in the  $\boldsymbol{\pi}$ -phase space. Choosing the dimensional constant  $\ell = \sqrt{\frac{\hbar}{eB}}$  (called magnetic length) as our unit of length and setting  $\hbar$  to unity, we

have  $[\pi_y, \pi_x] = i$ . Following standard treatment of the quantum SHO, we define creation and annihilation operators

$$b = \frac{\ell}{\sqrt{2}}(\pi_y + i\pi_x), \quad (1.7)$$

$$b^\dagger = \frac{\ell}{\sqrt{2}}(\pi_y - i\pi_x), \quad (1.8)$$

$$1 = [b, b^\dagger] \quad (1.9)$$

and recast the Hamiltonian in a familiar form

$$H = \omega_c \left( b^\dagger b + \frac{1}{2} \right), \quad (1.10)$$

where  $\omega_c = \frac{eB}{m}$  is the cyclotron frequency. Thus, the energy spectrum of this Hamiltonian is:

$$E_n = \omega_c \left( n + \frac{1}{2} \right). \quad (1.11)$$

These energy levels are called Landau levels. It also appears that the original problem with two degrees of freedom has been reduced to a simpler problem with only one degree of freedom. This indicates that the Landau levels must be highly degenerate. How can we describe this degeneracy arising from the missing degree of freedom?

It turns out that there are another set of gauge-invariant coordinates [8] that commute with  $\pi_i$  (and thus the kinetic energy), thus providing a way to describe states *within* a Landau level. These are the guiding center coordinates:

$$\mathbf{R} = \mathbf{r} + \frac{\ell^2}{\hbar} \hat{\mathbf{z}} \times \boldsymbol{\pi}.$$

One can check that (restoring our unit convention):

$$[R_i, \pi_j] = [x_i - \epsilon_{ik}\pi_k, \pi_j] = i(\delta_{ij} + \epsilon_{ik}\epsilon_{kj}) = 0, \quad (1.12)$$

$$\begin{aligned} [R_i, R_j] &= [x_i - \epsilon_{ik}\pi_k, x_j - \epsilon_{jl}\pi_l] = i(2\epsilon_{ij} - \epsilon_{kl}\epsilon_{ik}\epsilon_{jl}) \\ &= i\epsilon_{ij}. \end{aligned} \quad (1.13)$$

These guiding center components thus define a new quantized canonical phase space and provide the missing degree of freedom responsible for the degeneracy of Landau levels. Indeed, observing that energy eigenstates have zero averages for the  $\pi$ -components, we find  $\langle \mathbf{R} \rangle = \langle \mathbf{r} \rangle$ . Thus, the expectation value of the guiding center is nothing but the average location of the electron. Since the classical motion of electrons in a magnetic field takes the form of closed orbits known as cyclotron orbits, the gauge invariant variables directly describe the quantized versions of these classical objects. Note that this quantization is visually more appealing than the usual analysis of electronic motion in a magnetic field, which requires gauge fixing and eigenstates that look like long strips, very different from localized cyclotron orbits. For more details about this picture the reader is welcome to skip to Chapter 3, where we will also describe how the quantum Hall effect arises from combining the guiding center commutation relations and the classical drift of cyclotron orbits in crossed electric and magnetic fields.

#### 1.4 Microscopic origin of the fractional quantum Hall effect

The fractional quantum Hall states arise when we introduce interactions to the problem of a 2DEG in a perpendicular magnetic field. Consider the situation without interactions, but with the number of electrons such that the topmost Landau level is only partly full. The electrons in the partly filled topmost level can be rearranged in a macroscopic number of ways without changing the energy, thus the many-body ground state of the entire system is highly degenerate! This manifold of ground states is separated by an energy gap,  $\hbar\omega_c$ , from the excited states obtained by shifting electrons between different Landau levels.

When we incorporate interactions, the primary effect is that of splitting this large degeneracy of the many-body ground state manifold. This problem cannot be solved by naïve perturbation theory: because of the degeneracy, there is no relevant energy scale with respect to which the interaction is ‘small’, i.e., there is no small perturbation parameter. This problem is thus intrinsically ‘strongly correlated’. However, the quasi-one-dimensional nature of physics within a Landau level, as is evidenced by its essentially one-dimensional description in terms of the canonical phase space defined by the guiding center coordinates, leads to

(possibly complex) physics with apparently simple external manifestation: at specific filling fractions given by a restricted set of rational fractions, the ground state is gapped and possesses fractional Hall conductance. (Specifically, since cyclotron orbits drift with a universal speed of  $v = E/B$  perpendicular to the electric field, a gapped quantum Hall state with filling fraction  $\nu$  has a Hall conductance of simply  $\nu$  times that of a single Landau level, i.e., its Hall conductance is  $\sigma_H = \nu e^2/h$ .) The appearance of such strongly correlated gapped incompressible ground states at specific rational fractions can be captured by beautiful, though approximate, descriptions in terms of highly symmetric model wave functions. In the next chapter we will describe our contribution to improving tractability of this strongly correlated problem, using the appealing language of gauge-invariant variables.

We will now briefly describe Laughlin's seminal contribution, the formulation of a family of wave functions, that has motivated one of two widely used paradigms for understanding FQH physics via constructing model many-body wave functions. (The other paradigm is Jain's composite fermion approach[9].) Laughlin discovered an eponymous family of wave functions that describe FQH states occurring within the lowest Landau level (LLL), corresponding to filling factors of the form  $\nu = 1/p$ ,  $p$  being an odd integer.

Instead of choosing the Landau gauge as done previously in this Chapter, we will now choose the symmetric gauge to fix  $\mathbf{A}$ :  $\mathbf{A} = (\mathbf{B} \times \mathbf{r})/2$ . This makes the quadratic Hamiltonian explicitly rotationally symmetric. The wavefunctions are circular strips centered at the origin, with a very simple formula when considering states within the LLL:

$$\psi_m \propto z^m e^{-z\bar{z}/4}, \quad z = x + iy, m = 0, 1, 2, \dots \quad (1.14)$$

Thus, *any* single particle wavefunction in the LLL, in the symmetric gauge, can be written in the form  $\psi \sim f(z) e^{-z\bar{z}/4}$ , where  $f(z)$  is a holomorphic function. It follows that a multi-electron wave function in the LLL can be written as:

$$\Psi(z_1, z_2, \dots, z_N) \sim F(z_1, z_2, \dots, z_N) \times \text{Gaussian factor}, \quad (1.15)$$

where  $F$  is holomorphic in all arguments and also completely antisymmetric. This idea inspired Laughlin to propose the following series of wavefunctions as representing the topological properties of a family of FQH ground states:

$$\Psi_p(z_1, z_2, \dots, z_N) \sim \prod_{i < j} (z_i - z_j)^p \times \text{Gaussian factor}, \quad (1.16)$$

where  $p$  is an odd integer. Laughlin was able to find the properties of this wavefunction using ideas from plasma physics, deriving that this wave function corresponds to a uniform droplet with filling factor  $\nu = 1/p$  and providing evidence that it represents an incompressible state with fractionally charged quasiparticles whose charges are quantized at integer multiples of  $e/p$ . This wave function provides remarkably good agreement with numerical calculations involving a broad family of interactions and is widely accepted as describing the prominent FQH states at  $\nu = 1/3$  and  $1/5$ . Laughlin's approach has been followed up with novel constructions of FQH wavefunctions for many other filling fractions.

In the next Chapter we will show that such holomorphic construction of wavefunctions is not unique to the symmetric gauge or the LLL. Using the language developed therein, we will also derive an analytical form of the many-body Schrödinger's equation describing the dynamics of an interacting 2DEG in a magnetic field, projected into the ground state manifold of the corresponding non-interacting problem.

## 2. GAUGE-INVARIANT VARIABLES REVEAL THE QUANTUM GEOMETRY OF FRACTIONAL QUANTUM HALL STATES

In this Chapter, we will introduce the framework of gauge invariant variables (GIV) to describe fractional quantum Hall (FQH) states. To achieve this, we use the language of coherent states [10]–[14] to show that the many-body guiding-center wavefunction, which encapsulates the physics of FQH behavior, can be expressed in terms of holomorphic functions. As a special case, within the lowest Landau level, this function reduces to the well-known holomorphic coordinate representation of wavefunctions in the symmetric gauge.

Using this framework, we derive an analytic guiding center Schrödinger’s equation governing FQH states, which has a novel structure. We show how the electronic interaction is parametrized by generalized pseudopotentials, which depend on the Landau level occupancy pattern. In contrast to ad hoc holomorphic FQH ground state wavefunctions inspired by conformal blocks[4], [15], [16], our derivation of holomorphic many-body wave functions in higher Landau levels is first-principles-based and straightforward. As a special case, we find a simple relation between our holomorphic function and the well-known holomorphic function representation of real-space wavefunctions in the lowest Landau level [9], [17].

We finally functionalize this new language by deriving an analytic energy eigenvalue equation, Eq. (2.20), a qualitatively new form of the interacting many-body Schrödinger’s equation.

### 2.1 Gauge-invariant variables, again

As introduced in previous Chapter, we will be using the language of gauge-invariant variables (GIVs) to describe a 2DEG in a magnetic field. To motivate their use, we contrast with the conventional kinematic description of two-dimensional motion of particles using real-space coordinates and linear momenta (see Figure 2.1).

The intuition underlying the conventional description is that free particles should move in straight lines. Upon introducing a perpendicular magnetic field, the Lorentz force causes

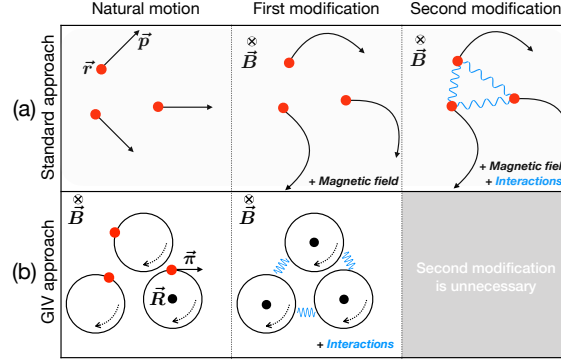


**Figure 2.1.** Comparing kinematic formulations of planar quantum mechanics in the presence of a magnetic flux,  $\mathbf{B}$ , using (a) conventional position and linear momentum, vs. (b) gauge-invariant variables (GIVs), namely, the kinetic momenta,  $\boldsymbol{\pi}$ , and the guiding center coordinates,  $\mathbf{R}$ . In (b), adding interactions is the only modification to the simple ‘free’ picture necessary, for describing strongly correlated fractional quantum Hall phases. In contrast, in (a), first the magnetic field needs to be incorporated and then interactions are added in.

these trajectories to bend into cyclotron orbits. Interactions add a second layer of complexity to the already-modified picture. Thus, the description of interacting particles in a magnetic field, namely, the physical situation where FQH states arise, is laborious in the conventional framework.

Our proposal to remedy this situation is to instead use a language which naturally includes the magnetic field in the ‘free’ picture, thus leaving us to deal only with the addition of interactions to the problem. This is accomplished by using GIVs. In this framework, the ‘free’ dynamical units are not the particles that move in straight lines, but rather, entire cyclotron orbits which are static in the absence of external fields (other than the background magnetic field). These orbits exhibit non-intuitive responses such as drifting perpendicularly to an in-plane electric field with a universal drift velocity  $E/B$  [17], [18]. This universal drift velocity is fundamentally related to the quantization of Hall conductance.



In what follows we consider electrons (with charge  $-e$ ) moving in an infinite flat plane. For this scenario, the GIVs are the well-known kinetic momenta and guiding center coordinates [8], respectively,

$$\boldsymbol{\pi} = \mathbf{p} + e\mathbf{A}(\mathbf{r}), \quad \mathbf{R} = \mathbf{r} + \left(\ell^2/\hbar\right) \hat{\mathbf{z}} \times \boldsymbol{\pi}. \quad (2.1)$$

Their commutation relation is

$$[R_i, \pi_j] = 0, \quad (2.2)$$

$$[R_i, R_j] = i\ell^2 \epsilon_{ij}. \quad (2.3)$$

The commutation relation of the guiding center coordinates captures the quantum geometry characterizing topological quantum systems. This is clear from analogous results in lattice systems [19] where this commutator has been related to the Chern number.

For brevity, in what follows we have set the magnetic length ( $\ell$ ), electronic charge ( $e$ ) and  $\hbar$  to unity. In these units, the commutation relations between the GIVs are analogous to the canonical commutation relations between the  $2D$  coordinates and canonical momenta:

$$[x, p_x] = i, \quad [y, p_y] = i, \quad [(x, p_x), (y, p_y)] = 0.$$

Thus, the GIVs can be obtained from canonical coordinates and momenta via a canonical transformation. Therefore, a unitary transformation relates the orthonormal quantum Hilbert space basis labeled by the coordinates,  $\{|x, y\rangle\}$ , to another labeled by  $\{|R_x, \pi_y\rangle\}$ , the values of one operator from each of the canonical pairs in Eq. (3.1). Consequently, the quantum wavefunction expressed in the GIV basis is a function of one component from each canonical pair in Eq. (3.1), for e.g.  $\psi(R_x, \pi_y)$ . By straightforward generalization, the form of the many-body electronic wavefunction in the GIV language is  $\Psi(\{R_x, \pi_y\}_1, \{R_x, \pi_y\}_2 \dots)$ , where the numerical subscripts label particles. This wavefunction is completely antisymmetric under the permutation of every particle pair.

## 2.2 GIV coherent states

Consider indexing the single-particle one-dimensional guiding center Hilbert space by an orthonormal basis  $\{|n\rangle\}$ , where  $n$  is a non-negative integer. Since the renormalized interaction potential,  $V$ , is rotationally invariant, we will choose the particular basis given by the eigenstates of  $\mathbf{R}^2$ :  $\mathbf{R}^2 |n\rangle = (2n + 1) |n\rangle$ . These states are simple harmonic oscillator states in guiding center space. They are also eigenstates of the projected interaction,  $V(\sqrt{2}|\mathbf{R}|) |n\rangle = V_n |n\rangle$ . The  $\{V_n\}$  are *generalized* pseudopotentials. For the special case when only one Landau level is considered, they reduce to the standard Haldane pseudopotentials [20]. If  $V$  has other symmetries, other choices for  $\{|n\rangle\}$  may be useful. Any quantum state in this Hilbert space can be uniquely expressed as a complex vector sum:  $|\psi\rangle = \sum_n \psi_n |n\rangle$ , with  $\sum_n |\psi_n|^2 = 1$ . The overcomplete basis of ‘coherent states’, labelled by the complex variable  $z$ , is defined as follows [10]–[14]:

$$|z\rangle = e^{-|z|^2/2} \sum_n \phi_n(z) |n\rangle, \quad \phi_n(z) = \frac{z^n}{\sqrt{n!}}. \quad (2.4)$$

The  $\{\phi_n\}$  are *holomorphic* functions whose choice above is motivated by the fact that we are considering motion in an infinite flat plane.  $e^{-|z|^2/2}$  is a normalizing factor. Due to the orthonormality of the  $\phi_n$  states,  $\iint_{\mathbf{C}} d^2z e^{-|z|^2} \phi_m^*(z) \phi_n(z) = \pi \delta_{mn}$ , the coherent states satisfy the well-known completeness relation:  $\iint_{\mathbf{C}} d^2z |z\rangle \langle z| = \pi \mathbf{I}$ <sup>1</sup>. Using the definition of coherent states, we can map *any* quantum state in guiding center space,  $|\psi\rangle = \sum_n \psi_n |n\rangle$ , to a unique holomorphic function:

$$\psi(z) \equiv e^{|z|^2/2} \langle \psi | z \rangle = \sum_n \psi_n^* \phi_n(z). \quad (2.5)$$

For simplicity, here we consider a single fractionally-filled Landau level and focus on the FQH physics induced by orbital interactions. The low-lying many-body energy eigenstates of such a partly filled Landau level are of the form

$$\Psi_m(\{(R_x, \pi_y)\}) = \eta(\pi_{y,1}) \eta(\pi_{y,2}) \dots \times \psi_m(\{R_x\}). \quad (2.6)$$

---

<sup>1</sup>For other useful properties of coherent states we refer the reader to [10]–[14].

In this expression the braces denote the set of all particle coordinates,  $\eta$  is the single particle Landau level kinetic momentum eigenfunction (it is a simple harmonic oscillator eigenfunction for isotropic dispersion [21], [22]) and  $\psi_m$  is a completely antisymmetric function. By over completeness of the tensor product coherent state  $|\{z_i\}\rangle$ , we can expand the  $\psi_m(\{R_x\})$  in terms of  $|\{z_i\}\rangle$ . Thus the wave function  $\Psi_m$  can be written in the form

$$\Psi_m = \eta(\pi_{y,1})\eta(\pi_{y,2}) \dots \times \psi_m(\{z_i\}), \quad (2.7)$$

where  $\psi_m(\{z_i\})$  is anti-symmetric in  $i$ .

Thus, the guiding center part of the wavefunction, whose properties are critical for uncovering FQH physics, can be described using holomorphic functions. This is true *irrespective of the filling fraction and which Landau levels are occupied*.

Our results have connections with the following known results. In the symmetric gauge, the quantum wavefunction in the lowest Landau level can be identified with a holomorphic function,  $\psi_0(z)$ , where  $z = x + iy$  (ignoring a fixed Gaussian factor) [9], [17]. This mathematical representation played a crucial role in identifying the Laughlin and related trial wavefunctions for FQH states in the lowest Landau level. An independent approach for generating real-space wavefunctions with desirable ground state characteristics involves using conformal blocks, which also give rise to approximately holomorphic functions [15], [16]. Our analysis demonstrates that holomorphic functions can also be used for describing states in the higher Landau levels, due to the quantum geometry encapsulated by the commutation properties of the guiding center GIVs. We have also identified the precise universal relationship between these holomorphic functions and the microscopic many-body wavefunction in the coordinate basis. As a special case, in the lowest Landau level, our holomorphic function in the coherent state representation,  $\psi$ , has a straightforward relation to the holomorphic wavefunction,  $\psi_0$ , in the *coordinate representation* in the symmetric gauge:  $\psi(z) = \psi_0(-i\sqrt{2}z^*)^*$ .

### 2.3 The Hamiltonian in GIV language

We consider the following interacting electronic many-body Hamiltonian in a magnetic field:

$$\mathcal{H} = \sum_{\alpha} K(\mathbf{p}_{\alpha} + \mathbf{A}(\mathbf{r}_{\alpha})) + \sum'_{\alpha\beta} U(|\mathbf{r}_{\alpha} - \mathbf{r}_{\beta}|). \quad (2.8)$$

The Greek indices label particles, and the prime on the second sum denotes a summation over distinct pairs.  $K$  and  $V$  are respectively the single-particle kinetic energy and the pairwise isotropic interaction potential.

The kinetic energy  $K(\mathbf{p} + \mathbf{A}(\mathbf{r})) \equiv K(\boldsymbol{\pi})$  is a function only of the kinetic momenta and has a discrete spectrum. These discrete energies correspond to the well-known Landau levels. The exact form of  $K$  and the presence of spin (or pseudospin) structure in the Hamiltonian do not alter our narrative. Thus, we will ignore distinctions between orbital and (pseudo)spin Landau level indices. In the absence of interactions, the single electron Hilbert space corresponding to a Landau level is extensively degenerate due to the freedom in choosing the guiding center part of the wavefunction, which does not affect the energy since  $\mathbf{R}$  commutes with  $\boldsymbol{\pi}$ .

When the topmost Landau level is partially filled, weak interactions split the macroscopic Landau-level degeneracy and give rise to FQH physics. In this regime, we can renormalize the interaction by averaging over the fast motion of kinetic momenta:

$$\begin{aligned} \langle U(|\mathbf{r}_{\alpha} - \mathbf{r}_{\beta}|) \rangle_{\boldsymbol{\pi}} &= \langle U(|\mathbf{R}_{\alpha} - \mathbf{R}_{\beta} + \hat{\mathbf{z}} \times (\boldsymbol{\pi}_{\alpha} - \boldsymbol{\pi}_{\beta})|) \rangle_{\boldsymbol{\pi}} \\ &\equiv V(|\mathbf{R}_{\alpha} - \mathbf{R}_{\beta}|). \end{aligned} \quad (2.9)$$

The renormalized interaction,  $V$ , depends on the Landau level structure and is a function only of the guiding center coordinates. This renormalization procedure involves *all* Landau levels and incorporates inter-Landau-level correlations, critical for accurately capturing the physics at higher fillings [23]. For the simple case when inter-Landau-level correlations are

neglected, and only the physics of the topmost Landau level is considered, this reduces to the Landau level projection technique [20]. Here we focus on the renormalized Hamiltonian:

$$\mathcal{H}_{\text{ren}} = \sum_{\alpha} K(\boldsymbol{\pi}_{\alpha}) + \sum'_{\alpha\beta} V(|\mathbf{R}_{\alpha} - \mathbf{R}_{\beta}|). \quad (2.10)$$

Since the kinetic and potential parts of this Hamiltonian commute, the energy eigenstates are products of Landau level kinetic momentum eigenfunctions of individual particles and a many-body wavefunction in guiding center space. When multiple Landau levels are involved, antisymmetrization entangles both GIV spaces in straightforward but complex ways, leading to interesting physics in states with filling fractions greater than one [9], [24], [25].

In this expression the braces denote the set of all particle coordinates,  $\eta$  is the single particle Landau level kinetic momentum eigenfunction (it is a simple harmonic oscillator eigenfunction for isotropic dispersion [21], [22]) and  $\psi_m$  is a completely antisymmetric eigenfunction of the effective interaction:

$$\left[ \sum'_{\alpha\beta} V(|\mathbf{R}_{\alpha} - \mathbf{R}_{\beta}|) \right] \psi_m \equiv \mathcal{U}_{\text{eff}} \psi_m = \epsilon_m \psi_m. \quad (2.11)$$

It is straightforward to incorporate the non-interacting energy contributed by the kinetic part,  $E_K$ . The many-body energies corresponding to  $\Psi_m$  are simply:

$$E_m = E_K + \epsilon_m. \quad (2.12)$$

The set  $\{\psi_m(\{R_x\}), \epsilon_m\}$  encodes the FQH physics arising due to interactions. This form also explicitly demonstrates that FQH physics is of a 1 + 1 dimensional nature, arising from guiding center dynamics [26]–[28].

## 2.4 GIV Schrödinger equation

We consider spinless electrons residing in the lowest Landau level. The kinetic momentum wavefunction is symmetric and the guiding center wavefunction completely antisymmetric under particle permutation. In terms of GIVs, the guiding center wavefunction corresponds

to a single antisymmetric holomorphic function  $\psi(\{z\})$ . The number of arguments equals the number of particles in the partly-filled Landau level.

We now present how the GIV holomorphic representation can be put to practical use, by deriving the corresponding Schrödinger equation for determining the energy eigenstates. This is achieved by expressing Eq. (2.11) in the coherent state representation,  $\langle\psi|\mathcal{U}_{\text{eff}}|\{z\}\rangle = \epsilon\langle\psi|\{z\}\rangle = \epsilon\psi(\{z\})$ .

Consider the pairwise interaction operator,  $V(|\mathbf{R}_i - \mathbf{R}_j|)$ , which is an isotropic function of the difference of guiding center coordinates of particles ‘ $i$ ’ and ‘ $j$ ’. Denote the components of the guiding center coordinates,  $\mathbf{R}$ , by  $(X, Y)$ . The components of  $\mathbf{R}_{\pm} = (X_i \pm X_j, Y_i \pm Y_j)/\sqrt{2}$  are also canonical pairs, which commute between the  $\pm$  labels, in the same sense as the guiding center coordinates  $\mathbf{R}_{i,j}$ . The corresponding annihilation operators are  $A_{\pm} = (a_i \pm a_j)/\sqrt{2}$ , where  $a_i$  is the annihilation operator for the coherent states generated for the guiding center variables  $\mathbf{R}_j$ . Consequently,  $a_{i,j} = (A_+ \pm A_-)/\sqrt{2}$ . The vacuum state,  $|0\rangle_{\pm}$ , defined via annihilation by both  $A_{\pm}$  is the same as  $|0\rangle_{ij}$ , the vacuum state defined via annihilation by both  $a_{i,j}$ .

The eigenstates of the interaction  $V(|\mathbf{R}_i - \mathbf{R}_j|) = V(\sqrt{2}|\mathbf{R}_-|)$  are the SHO states in the guiding coordinate Hilbert space, since they are the same as the eigenstates of  $\mathbf{R}_-^2$ . The eigenvalues of  $V(\sqrt{2}|\mathbf{R}_-|)$  are the Haldane pseudopotentials,  $\{V_n\}$ . The annihilation operator relating the eigenstates are given by  $A_- \propto X_- + iY_-$ . The corresponding coherent states are  $|z\rangle_- = e^{zA_-^\dagger - z^*A_-}|0\rangle_-$ , where the vacuum state is defined through  $A_-|0\rangle_- = 0$ .

Any coherent state defined through  $\mathbf{R}_{i,j}$  is equal to another coherent state in the  $\pm$  basis:

$$\begin{aligned} |z_i, z_j\rangle_{i,j} &= e^{z_i a_i^\dagger - z_i^* a_i} e^{z_j a_j^\dagger - z_j^* a_j} |0\rangle_{ij} = e^{\left(\frac{z_i + z_j}{\sqrt{2}}\right) A_+^\dagger - \left(\frac{z_i + z_j}{\sqrt{2}}\right)^* A_+} e^{\left(\frac{z_i - z_j}{\sqrt{2}}\right) A_-^\dagger - \left(\frac{z_i - z_j}{\sqrt{2}}\right)^* A_-} |0\rangle_{\pm} \\ &= \left| \frac{z_i + z_j}{\sqrt{2}}, \frac{z_i - z_j}{\sqrt{2}} \right\rangle_{+-} \equiv |z_+, z_-\rangle_{+-}. \end{aligned} \quad (2.13)$$

This is a remarkable result. In addition, the unnormalized coherent states, defined as  $||z\rangle = e^{|z|^2/2} |z\rangle$ , are also equal,

$$||z_i, z_j\rangle_{i,j} = \left\| \frac{z_i + z_j}{\sqrt{2}}, \frac{z_i - z_j}{\sqrt{2}} \right\rangle_{+-} \equiv ||z_+, z_-\rangle_{+-}. \quad (2.14)$$

We can also write:

$$\langle w_- || V(|\mathbf{R}_i - \mathbf{R}_j|) || z_- \rangle = \langle w_- || V(\sqrt{2}|\mathbf{R}_-|) || z_- \rangle = \sum_{n=0}^{\infty} \frac{V_n}{n!} (w_-^* z_-)^n \equiv \tilde{V}(w_-^* z_-). \quad (2.15)$$

Here,  $V_n$  are the generalized pseudopotentials.

By the coherent state overlap formula  $\langle w || | z \rangle = e^{w^* z}$ , we find that

$$\begin{aligned} \langle w_i, w_j || V(|\mathbf{R}_i - \mathbf{R}_j|) || z_i, z_j \rangle &= \langle w_+, w_- || V(|\mathbf{R}_i - \mathbf{R}_j|) || z_+, z_- \rangle = e^{w_+^* z_+} \tilde{V}(w_-^* z_-) \\ &= e^{w_+^* z_+} \sum_{n=0}^{\infty} \frac{V_n}{n!} (w_-^* z_-)^n. \end{aligned} \quad (2.16)$$

Every many-body guiding center quantum state,  $|\psi\rangle$ , corresponds to a multivariate analytic function,  $\psi(z_1, z_2, \dots) = \langle \psi || z_1, z_2, \dots \rangle$ , in analogy to the single particle state. For identical particles in the same Landau level, this function should be either completely symmetric (Bosons) or antisymmetric (Fermions).

Denoting  $V(|\mathbf{R}_i - \mathbf{R}_j|) \rightarrow V_{ij}$ , the action of the full many-body potential,  $\mathcal{U}_{\text{eff}} = \sum_{i < j} V_{ij}$ , on a many-body wavefunction can be calculated using Eq. (2.16).

$$\langle \psi | \mathcal{U}_{\text{eff}} || \{z\} \rangle = \sum_{n=0}^{\infty} \sum_{i < j} \frac{V_n}{n!} \iiint \{d\mu(w)\} \psi(\{w\}) e^{\sum_{k \neq (i,j)} w_k^* z_k} e^{w_+^* z_+} (w_-^* z_-)^n, \quad (2.17)$$

where we have used the general shorthand  $\xi_{\pm} = (\xi_i \pm \xi_j)/\sqrt{2}$  and introduced the integration measure on the complex plane,  $d\mu(z) = d^2 z e^{-|z|^2}/\pi$ .

Using standard identities for coherent states, we simplify the integral appearing in the sum above, for a fixed value of  $(n, i, j)$ , as follows ( $k \neq (i, j)$  in all expressions below):

$$\begin{aligned}
& \iiint \{d\mu(w)\} \psi(\{w\}) e^{\sum_{k \neq (i,j)} w_k^* z_k} e^{w_+^* z_+} (w_-^* z_-)^n \\
&= (-1)^{K_{ij}} \iint d\mu(w_i) d\mu(w_j) \psi(w_i, w_j, \{z_k\}) e^{w_+^* z_+} (w_-^* z_-)^n \\
&= (-1)^{K_{ij}} \left( \frac{\partial}{\partial \lambda} \right)^n \iint d\mu(w_i) d\mu(w_j) \psi(w_i, w_j, \{z_k\}) e^{w_+^* z_+ + \lambda w_-^* z_-} \Big|_{\lambda=0} \\
&= (-1)^{K_{ij}} \left( \frac{\partial}{\partial \lambda} \right)^n \iint d\mu(w_+) d\mu(w_-) \psi \left( \frac{w_+ + w_-}{\sqrt{2}}, \frac{w_+ - w_-}{\sqrt{2}}, \{z_k\} \right) e^{w_+^* z_+ + \lambda w_-^* z_-} \Big|_{\lambda=0} \\
&= \left( \frac{\partial}{\partial \lambda} \right)^n \psi \left( \left\{ \xi_k = z_k, \xi_i = \frac{z_+ + \lambda z_-}{\sqrt{2}}, \xi_j = \frac{z_+ - \lambda z_-}{\sqrt{2}} \right\} \right) \Big|_{\lambda=0} \\
&= \left( \frac{z_-}{\sqrt{2}} \left[ \frac{\partial}{\partial \xi_i} - \frac{\partial}{\partial \xi_j} \right] \right)^n \psi(\{\xi\}) \Big|_{\{\xi_k = z_k, \xi_i = \xi_j = z_+/\sqrt{2}\}} \tag{2.18}
\end{aligned}$$

In the above expression,  $(-1)^{K_{ij}} \psi$  is a function that arises from moving the  $z_{i,j}$  variables to the first two slots of  $\psi$  (it is introduced to simplify notation and plays no significant role) and we have used the remarkable fact that  $d\mu(w_i) d\mu(w_j)$  is equal to  $d\mu(w_+) d\mu(w_-)$ .

Thus,

$$\langle \psi | \mathcal{U}_{\text{eff}} | \{z\} \rangle = \sum_{n=0}^{\infty} \frac{V_n}{n!} \sum_{i < j} \left( \frac{z_i - z_j}{2} \right)^n \left( \frac{\partial}{\partial \xi_i} - \frac{\partial}{\partial \xi_j} \right)^n \psi(\{\xi\}) \Big|_{\{\xi_k = z_k, \xi_i = \xi_j = \frac{z_i + z_j}{2}\}}. \tag{2.19}$$

The eigenvalue equation,  $\mathcal{U}_{\text{eff}} |\psi\rangle = \epsilon |\psi\rangle$ , thus yields the GIV Schrödinger's equation in the main text:

$$\sum_{n=0}^{\infty} \frac{V_n}{n!} \sum_{i < j} \left( \frac{z_i - z_j}{2} \right)^n \left( \frac{\partial}{\partial \xi_i} - \frac{\partial}{\partial \xi_j} \right)^n \psi(\{\xi\}) \Big|_{\{\xi_k = z_k, \xi_i = \xi_j = \frac{z_i + z_j}{2}\}} = \epsilon \psi(\{z\}). \tag{2.20}$$

This equation is *valid for any filling fraction*, including cases when there are other completely filled Landau levels in the picture. In the context of coordinate basis wavefunctions, applicable only to the lowest Landau level, such an operator representation has appeared previously in [29]. The GIV Schrödinger equation, Eq. (2.20), is also applicable to higher Landau levels. The simple form of this result reflects the projection Hamilton used: we have



ignored particle-hole excitations involving the filled lower and empty higher Landau levels, an assumption relevant for most observed fractional quantum Hall states [4], [30].

## 2.5 Example: Laughlin state

To illustrate how Eq. (2.20) can be utilized, we derive the following well known result: the Laughlin state at filling fraction  $\nu = 1/m$  is the exact unique most compact ground state when the first  $m - 1$  pseudopotentials ( $V_1, V_2 \dots V_{m-1}$ ) are positive and the rest are zero.

The operator  $\hat{L}_n^{ij}$  multiplying the pseudopotential  $V_n$  in Eq. (2.20) is a *projection operator*

$$\hat{L}_n^{ij} \psi(\{z\}) = \frac{1}{n!} \left( \frac{z_i - z_j}{2} \right)^n \left( \frac{\partial}{\partial \xi_i} - \frac{\partial}{\partial \xi_j} \right)^n \psi(\{\xi\}) \Big|_{\left\{ \xi_k = z_k, \xi_i = \xi_j = \frac{z_i + z_j}{2} \right\}}. \quad (2.21)$$

which satisfies relation  $(\hat{L}_n^{ij})^2 = \hat{L}_n^{ij}$ . By the definition of this operator, it selects out the coefficient of  $(z_i - z_j)^n$ . Since projection operators have eigenvalues 0 or 1, a sum of projection operators with positive coefficients also has a non-negative expectation value.

Any antisymmetric holomorphic function  $\psi(\{z\})$  must be of the form

$$\psi_P(\{z\}) = \Delta^m P(\{z\})$$

where  $m$  is an odd integer,  $\Delta = \Pi_{i < j} (z_i - z_j)$  is the Vandermonde determinant and  $P$  is an arbitrary symmetric polynomial. This is because for any antisymmetric polynomial it contains all zeros of the form  $(z_i - z_j)$  hence the polynomial factors at least for one power of Vandermonde determinant, and since both  $\psi_P(\{z\})$  and  $\Delta^m$  are antisymmetric,  $P$  must be symmetric.

The Hamiltonian of the form  $H = \sum_{k < m-1} V_k \sum_{i < j} L_k^{ij}$  with  $V_k > 0$  has positive expectation values (because  $V_k$  are positive and  $L_k^{ij}$  has positive expectation values), then the minimal possible eigenvalue of  $H$  must be non-negative. Then by the natural of operator  $\hat{L}_n^{ij}$  and antisymmetric polynomial of the form  $\psi_P(\{z\}) = \Delta^m P(\{z\})$ , we see that for  $H \cdot \psi_P(\{z\}) = 0$ . So the polynomial of the form  $\psi_P(\{z\}) = \Delta^m P(\{z\})$  has to be a ground state.

We now define the filling fraction in the usual way for a droplet geometry. Following the definition of coherent states in the main text, since the power  $z^n$  corresponds to an orbital defined at the guiding center radius  $|R| = \sqrt{2n+1}$ , the filling fraction of the polynomial  $\psi(\{z\})$  should be calculated with respect to a droplet whose radius corresponds to the highest individual power in  $\psi(\{z\})$ . Thus, increasing the polynomial degree of  $P$  increases the size of the droplet, which corresponds to a decreasing filling fraction since  $N$  is fixed. Among the manifold of zero energy states  $\psi_P(\{z\})$ , the filling fraction reaches its maximum value (the wavefunction reaches its most spatially compact form) when the polynomial  $P$  is a constant (with the least possible degree of zero). Then for the given Hamiltonian, the unique compact ground state is  $\Delta^m$ , i.e. the Laughlin wavefunction. The filling fraction is  $\nu = 1/m$ , in the limit of an infinite number of particles.

## 2.6 Summary

We have used the language of GIVs to derive a holomorphic representation of FQH physics, which is valid for *any* Landau level filling pattern and for arbitrary forms of the kinetic energy. The framework that we have developed can be generalized to accommodate a variety of scenarios involving different real space manifolds and symmetries. We have then considered the important case in which only one Landau level is partly filled and all other levels are either full or empty. For this case we have shown that the quantum state can be expressed by a single antisymmetric holomorphic function in the GIV coherent state basis. Formulating the FQH problem in this language, on an infinite plane with arbitrary isotropic pairwise interactions, ignoring all high-energy processes in the form of particle-hole excitations between Landau levels, we have derived the analytic GIV Schrödinger equation, Eq. (2.20). The FQH many-body ground and excited state wavefunctions and energies correspond to the eigenstates and eigenvalues of this novel eigenvalue equation.

Eq. (2.20) provides a new route for deriving the properties of FQH states from microscopic Hamiltonians, by recasting the quantum many-body calculation in the GIV representation. Since the wavefunction corresponds to an antisymmetric holomorphic function, our formulation also provides an avenue to exploit insights from diverse mathematical fields such as

symmetric polynomials[31], complex analysis, etc. We hope that a synthesis of our formalism with these techniques will provide an accessible route for first-principles based predictions of FQH state properties, starting from realistic microscopic Hamiltonians. Apparently distinct descriptions of FQH physics, such as trial holomorphic wavefunctions in the lowest Landau level [3], [9]; variational Laughlin wavefunctions describing the collective modes [32], [33]; the conformal block picture from conformal field theory [15], [16]; the composite fermion approach [9]; topological quantum field theory [34]; and matrix product states [35] may be naturally unified in our coherent state GIV formulation in future works.

### 3. GEOMETRIC RESPONSE OF QUANTUM HALL STATES TO ELECTRIC FIELDS

Quantum Hall states [1], [2] were the first examples and paradigmatic models of topological quantum states of matter [36], [37] whose defining characteristic is the topologically protected quantization of their eponymous conductance property. Less well known is the quantization of their gravitational coupling constant, which characterizes charge response to spatial curvature in the continuum [38] and on lattices [39]. There is an active quest to understand the topological protection of the gravitational coupling constant in terms of fundamental physical principles [40]. There have been researches using effective topological field theory techniques, finding that the gravitational coupling constant is proportional to the anomalous viscosity [41], [42] and appears in the current response to non-uniform electric fields [43].

In this Chapter, we address the connection between gravitational coupling, local charge response to nonuniform electric fields and anomalous viscosity. We provide tangible connections between the response of quantum Hall fluids to non-uniform electric fields, and the characteristic geometry of electronic motion in the presence of magnetic and electric fields. The geometric picture we provide motivates the following conjecture: non-uniform electric fields mimic the presence of spatial curvature. Consequently, the gravitational coupling constant also appears in the charge response to non-uniform electric fields.

To elucidate the characteristic geometry of electronic motion in a magnetic field we will be using the explicitly gauge-invariant variables of Hall system, i.e. the kinetic momentum and guiding center coordinates, and thus a calculational framework naturally suited for describing attendant physics. Our formulation is based on the semiclassical description of quantum Hall physics in terms of gauge invariant variables, and using phase space representation of quantum mechanics (Wigner functions, Moyal formalism). We will be focusing on the single particle physics of electrons in the presence of a magnetic field, and present a calculation to conceptualize the shearing of cyclotron orbits in the presence of non-uniform electric fields (Figure 3.1). We find that the Hall viscosity contribution in the current response [41], [43] is a direct consequence of shearing of cyclotron orbits. Our formalism directly

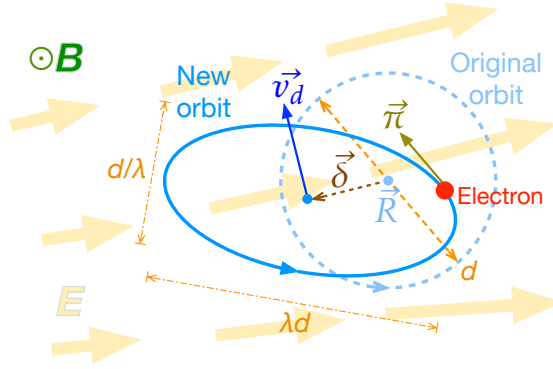


**Figure 3.1.** A geometric summary of how a non-uniform electric field,  $\mathbf{E}$ , deforms a cyclotron orbit. The changes can be expressed in terms of a vector field,  $\Delta(\mathbf{R})$  (Eq. (3.25b)), and a shearing field,  $\Lambda(\mathbf{R})$  (Eq. (3.28b)). The new orbit is shifted by amount  $\delta(\mathbf{R}) = \hat{z} \times \Delta(\mathbf{R})$  with respect to the original center,  $\mathbf{R}$ , and acquires a drift velocity,  $\mathbf{v}_d = \Delta(\mathbf{R})$ . The orbit is also sheared into an ellipse with aspect ratio  $\lambda^2$ ; see Eq. (3.34) and accompanying text for details. The guiding center coordinate,  $\mathbf{R}$ , labels the field-free orbit center while the kinetic momentum,  $\boldsymbol{\pi}$ , gives the velocity of the electron (Eq. (2.1)).

connects the shearing of cyclotron orbits, i.e., a change in the effective Galilean metric, to the non-uniformity of electric fields. We calculate the effective spatial curvature induced by the electric field, Eq. (3.26) and predict that the gravitational response of integer quantum Hall states also appears in the charge response to non-uniform electric fields. We confirm our predictions with numerical calculations and conclude with a conjecture regarding the extension of these results to fractional quantum Hall states.

### 3.1 Wavefunctions in the GIV formalism

For brevity, we set the magnetic length ( $\ell$ ), electronic charge ( $e$ ) and  $\hbar$  to unity. In places where we consider a specific Hamiltonian we assume a quadratic dispersion for electrons with unit mass ( $m$ ) and ignore the effects of spin.

The commutation relations between the GIVs [8],

$$[R_x, R_y] = i, \quad [\pi_y, \pi_x] = i, \quad [\pi_i, R_j] = 0, \quad (3.1)$$

are canonical and analogous to the canonical commutation relations between the  $2D$  coordinates and canonical momenta:

$$[x, p_x] = i, \quad [y, p_y] = i, \quad [(x, p_x), (y, p_y)] = 0. \quad (3.2)$$

Thus, the GIVs can be obtained from the canonical coordinates and momenta via a canonical transformation: a unitary transformation exists from the orthonormal quantum Hilbert space basis labeled by the coordinates,  $\{|x, y\rangle\}$ , to another labeled by the values of one operator from each of the canonical pairs in Eq. (3.1). For example,  $\{|R_x, \pi_y\rangle\}$ , labeled by the eigenvalues of the operators  $(R_x, \pi_y)$ , form one such orthonormal basis. It is well known that the Hilbert space can be labeled by any of the following orthonormal bases:  $\{|p_x, y\rangle\}$ ,  $\{|x, p_y\rangle\}$ , or  $\{|p_x, p_y\rangle\}$ . Analogously, alternate GIV representations are possible:  $\{|R_y, \pi_x\rangle\}$ ,  $\{|R_x, \pi_x\rangle\}$  or  $\{|R_y, \pi_y\rangle\}$ .

To illustrate use of this formalism, we derive the unitary transformation matrix elements  $\langle x, y | R_x, \pi_y \rangle \equiv \chi(x, y)$ , i.e., the wave function of a GIV basis state in the conventional coordinate (Schrödinger) representation. By definition,  $\chi(x, y)$  is the simultaneous eigenstate of  $\hat{R}_x$  and  $\hat{\pi}_y$ , with eigenvalues  $R_x$  and  $\pi_y$  respectively. Since the coordinate representation is gauge-dependent, we will need to choose a gauge for the magnetic vector potential,  $\mathbf{A}$ . First, we consider the Landau gauge,  $\mathbf{A}_{\text{Lan}} = x\hat{\mathbf{y}}$  (note that  $B = 1$  in our units). The eigenvalue conditions become:

$$i\partial_y\chi = R_x\chi, \quad -i\partial_y\chi + x\chi = \pi_y\chi. \quad (3.3)$$

The (unnormalized) solution is

$$\chi_{\text{Lan}}(x, y) \propto \delta(x - R_x - \pi_y)e^{-iR_xy}. \quad (3.4)$$

Alternately, we can find  $\chi(x, y)$  in the symmetric gauge,  $\mathbf{A}_{\text{sym}} = (-y\hat{\mathbf{x}} + x\hat{\mathbf{y}})/2$ :

$$\chi_{\text{sym}}(x, y) \propto \delta(x - R_x - \pi_y)e^{-iR_xy}e^{i\frac{xy}{2}}. \quad (3.5)$$

Despite the necessity to gauge-fix  $\{|x, y\rangle\}$ , the GIV states  $\{|R_x, \pi_y\rangle\}$  are themselves invariant under gauge transformations. Consequently,  $\chi_{\text{Lan}}$  and  $\chi_{\text{sym}}$  differ only by a GIV-independent phase factor; the corresponding phase,  $\phi = xy/2$ , satisfies  $\nabla\phi = \mathbf{A}_{\text{Lan}} - \mathbf{A}_{\text{sym}}$ .

Within the GIV formalism, now consider the energy eigenstates of an electron in  $2D$  experiencing a perpendicular magnetic field. Assuming minimal coupling to the gauge field, the Hamiltonian is of the form:

$$\mathcal{H} = K(\mathbf{p} + e\mathbf{A}) - V(\mathbf{r}) \equiv K(\boldsymbol{\pi}) - V(\mathbf{R} + \boldsymbol{\pi} \times \hat{\mathbf{z}}). \quad (3.6)$$

Here,  $K$  denotes the kinetic operator.  $V$  is the local electrostatic potential which includes contributions both from externally applied fields and local electrostatic irregularities in the material; the negative sign results from the sign of electronic charge. When  $V = 0$ , since the Hamiltonian is only a function of the kinetic momenta, the eigenstates in the GIV basis  $\{|R_x, \pi_y\rangle\}$  can be found by separation of variables:

$$\Psi(R_x, \pi_y) = \psi(R_x)\eta(\pi_y). \quad (3.7)$$

For quadratic dispersion,  $K(\boldsymbol{\pi}) = \boldsymbol{\pi}^2/2$ , the commutation relations, Eq. (3.1), imply that the Hamiltonian is equivalent to that of a quantum simple harmonic oscillator with energies<sup>1</sup> and eigenfunctions<sup>2</sup> of the form:

$$\begin{aligned} K(\boldsymbol{\pi})\eta_n(\pi_y) &= \chi_n\eta_n(\pi_y), \quad n = 0, 1, \dots, \\ \chi_n &= n + \frac{1}{2}, \quad \eta_n(\pi_y) = \frac{e^{-\pi_y^2/2} H_n(\pi_y)}{\sqrt{2^n n! \sqrt{\pi}}}. \end{aligned} \quad (3.8)$$

Thus, the discrete nature of the eigenvalue spectrum of  $K(\boldsymbol{\pi})$  arises from the commutation relations satisfied by the kinetic momenta GIVs and defines the familiar electronic Landau levels (LLs). The kinetic operator does not affect the guiding center part of the wavefunction,  $\psi(R_x)$ , an arbitrary function, resulting in the high degeneracy of the Landau levels.

---

<sup>1</sup><http://dlmf.nist.gov/18.39.E4>

<sup>2</sup><http://dlmf.nist.gov/18.39.E5>

This degeneracy is countable; the countability arises from the canonical commutation relation satisfied by the guiding center variables. This degeneracy can be counted using von Neumann's result that the phase space density of quantum states is  $(2\pi)^{-1}$  [44]. Thus, in the guiding center phase space, i.e., the  $2D$  space spanned by  $(R_x, R_y)$ , there is one quantum state corresponding to each area of  $2\pi$ . This area corresponds to an equal area in real space, since the guiding center corresponds to the real-space location of the cyclotron orbit center. Putting together these results and restoring units, we arrive at the well-known result: inside a Landau level, there is an extensive degeneracy arising from the existence of one quantum state per real space area of  $2\pi\ell^2 = (h/e)/B$ , i.e., the area pierced by one flux quantum,  $\phi_0 = h/e$ .

The gauge-invariant nature of the GIV quantum basis allows for straightforward visualization and representation of Landau level wavefunctions. The popularly-used wavefunctions in the Landau ( $L$ ) and symmetric ( $S$ ) gauges in the LL with index  $n$  become simply [17]:

$$\Psi_L = \delta(R_x - X)\eta_n(\pi_y), \quad (3.9)$$

$$\Psi_S = \eta_m(R_x)\eta_n(\pi_y). \quad (3.10)$$

These are respectively parametrized by  $X$ , the  $x$ -coordinate of the guiding center, and  $m = 0, 1, \dots$ , the eigenvalue of the operator  $(R_x^2 + R_y^2 - 1)/2$ . Note that the kinetic momentum-dependent part of the wavefunction is the same for both: it is fixed for a given LL. Thus written, these wavefunctions are gauge-independent. The corresponding Schrödinger wavefunctions in *any* gauge can be calculated using the appropriate unitary transformation. It is straightforward to convert  $\Psi_S$ , the conventional wavefunctions used in the symmetric gauge, to the Landau gauge using the unitary transform derived in Eq. (3.4):

$$\begin{aligned} \Psi_S(x, y) &= \iint dR_x d\pi_y \chi(x, y) \eta_m(R_x) \eta_n(\pi_y) \\ &\propto e^{-\frac{x^2 + y^2 - 2ixy}{4}} (x - iy)^{n-m} L_m^{n-m} \left( \frac{x^2 + y^2}{2} \right). \end{aligned} \quad (3.11)$$



Here,  $L_n^\alpha$  are the associated Legendre polynomials<sup>3</sup>. This result can be verified by straightforward computation of the integral. Comparison with conventional wavefunctions in the circular gauge [17] shows that the above expression differs only by a factor of  $e^{ixy/2}$ . This is as expected since the gradient of  $xy/2$  accounts for the difference between the symmetric and Landau gauge vector potentials.

### 3.2 Motion in a non-uniform electric field

Consider the general Hamiltonian with quadratically dispersing kinetic energy, which describes electronic motion in the presence of crossed uniform magnetic and *non-uniform* electric fields:

$$\mathcal{H} = \frac{(\mathbf{p} + \mathbf{A})^2}{2} - V(\mathbf{r}) \equiv \frac{\boldsymbol{\pi}^2}{2} - V(\mathbf{R} + \boldsymbol{\pi} \times \hat{\mathbf{z}}). \quad (3.12)$$

Our objective in this section is to calculate the local charge and current density operators as linear gradient expansions in the electrostatic potential  $V$ . We will also relate a subset of these expansion coefficients to apparently unrelated topological quantities, which describe electronic response to geometrical real space (gravitational) perturbations to cyclotron motion [38], [43]. The local charge and current operators are expressed in terms of the GIVs as follows. (Operators have been distinguished from  $c$ -numbers using carets in what follows. However,  $\hat{\mathbf{z}}$  is the unit vector along the  $z$ -direction.)

$$\hat{\rho}(\mathbf{r}) = \delta(\hat{\mathbf{r}} - \mathbf{r}) = \delta(\hat{\mathbf{R}} + \hat{\boldsymbol{\pi}} \times \hat{\mathbf{z}} - \mathbf{r}), \quad (3.13a)$$

$$\hat{\mathbf{j}}(\mathbf{r}) = \frac{\{\hat{\mathbf{v}}, \delta(\hat{\mathbf{r}} - \mathbf{r})\}}{2} = \frac{\{\boldsymbol{\pi}, \delta(\hat{\mathbf{R}} + \hat{\boldsymbol{\pi}} \times \hat{\mathbf{z}} - \mathbf{r})\}}{2}. \quad (3.13b)$$

Here  $\hat{\mathbf{v}} = i[\mathcal{H}, \mathbf{r}] = \hat{\boldsymbol{\pi}}$  is the velocity operator.

We assume that the potential  $V$  is weak and varies slowly in space; specifically, that its variation over a magnetic length is negligible compared to the inter-Landau level energy gap. This condition needs to be satisfied for the electronic motion to exhibit topological

---

<sup>3</sup><http://dlmf.nist.gov/18.5.E12>

transport properties of the associated Landau level. In chosen units the inter-Landau level energy gap is unity. (It is equal to  $\hbar\omega_c$ , where  $\omega_c = eB/m = 1$  is the cyclotron frequency, i.e., the angular frequency of classical cyclotron motion.) Thus, the condition that  $V$  is weak and slowly varying is equivalent to the following set of conditions in our chosen units:

$$\partial_{\mathbf{r}}^m V(\mathbf{r}) \ll 1, \quad m = 1, 2, \dots \quad (3.14)$$

The condition on  $V$  can be used to approximate the operator,  $V(\mathbf{r})$ , by the first few terms of the Taylor series,

$$\begin{aligned} V(\mathbf{r}) &\equiv V(\mathbf{R} + \boldsymbol{\pi} \times \hat{\mathbf{z}}) \\ &= V(\mathbf{R}) + (\partial_a V(\mathbf{R})) (\epsilon_{ap} \pi_p) + \frac{1}{2} (\partial_{ab}^2 V(\mathbf{R})) (\epsilon_{ap} \epsilon_{bq} \pi_p \pi_q) \\ &\quad + \frac{1}{6} (\partial_{abc}^3 V(\mathbf{R})) (\epsilon_{ap} \epsilon_{bq} \epsilon_{cr} \pi_p \pi_q \pi_r) + \dots \end{aligned} \quad (3.15)$$

We have used the Einstein convention for summation of repeated indices (over the two values  $x$  and  $y$ ) and the two dimensional Levi-Civita tensor  $\epsilon_{xx} = \epsilon_{yy} = 0$ ,  $\epsilon_{xy} = -\epsilon_{yx} = 1$ . This decomposition has two-fold utility. First, the derivatives of  $V$  are all small since  $V$  is weak and slowly varying, thus allowing for the use of perturbation theory to calculate modifications to the cyclotron motion. Second, within a Landau level the kinetic momenta,  $(\pi_x, \pi_y)$ , are rapidly oscillating relative to each other since they form a canonical pair governed by the SHO Hamiltonian,  $K(\boldsymbol{\pi}) = (\pi_x^2 + \pi_y^2)/2$ . Consequently, the products of kinetic momentum operators in the above expansion are either rapidly varying or static, thus allowing for a clear separation of time scales.

### 3.2.1 Landau-level projection

In light of the Taylor expansion in Eq. (3.15), the simplest tractable approximation to the full Hamiltonian, Eq. (3.12), involves neglecting all perturbative terms in Eq. (3.15). This

crude approximation is equivalent to the standard procedure of Landau-level projection. Within this approximation, the eigenstates of Eq. (3.12) can be written in the form:

$$\Psi_{m,n}(\mathbf{R}_x, \pi_y) = \psi_m(R_x) \eta_n(\pi_y), \quad E_{m,n} = \chi_n + v_m, \quad (3.16)$$

where  $\eta_n$  and  $\chi_n$  are SHO eigen wavefunction and eigen energies

$$\begin{aligned} K(\boldsymbol{\pi}) \eta_n(\pi_y) &= \chi_n \eta_n(\pi_y), \quad n = 0, 1, \dots, \\ \chi_n &= n + \frac{1}{2}, \quad \eta_n(\pi_y) = \frac{e^{-\pi_y^2/2} H_n(\pi_y)}{\sqrt{2^n n! \sqrt{\pi}}}. \end{aligned} \quad (3.17)$$

where  $H_n$  are hermitian polynomials and the guiding center eigenfunctions are determined by

$$V(\hat{\mathbf{R}}) |\psi_m\rangle = -v_m |\psi_m\rangle. \quad (3.18)$$

This eigenequation is unusual because both canonically conjugate operators,  $\hat{R}_x$  and  $\hat{R}_y$ , are a priori present with equal priority in  $V$ . However, the nature of the eigenfunctions can be deduced from the well-known operator equations of motion:

$$\dot{\mathbf{R}} = i [\mathcal{H}, \mathbf{R}] = \hat{\mathbf{z}} \times \boldsymbol{\nabla} V(\mathbf{r}) = -\hat{\mathbf{z}} \times \mathbf{E}(\mathbf{r}), \quad (3.19)$$

where  $\mathbf{E}(\mathbf{r}) = -\boldsymbol{\nabla} V(\mathbf{r})$  is the local electric field. Using our Landau-level projection approximation,  $\mathbf{r} \sim \mathbf{R}$  and so  $\dot{\mathbf{R}} \simeq -\hat{\mathbf{z}} \times \boldsymbol{\nabla} V(\mathbf{R})$ , which implies that cyclotron orbits drift along equipotentials [17]. Consequently the (stationary) eigenstates of Eq. (3.18) should also lie along equipotentials and each cover an area of  $2\pi\ell^2$ .

In the presence of a random disorder potential with short range correlations, equipotentials are closed in the bulk, thus localizing all bulk states as shown in Figure 3.2. The boundary, assumed to be a steep confining potential, has extended wavefunctions circulating along the perimeter. These are the so-called edge states [45]. What we have described here is the standard non-interacting picture of bulk localization in a magnetic field. This accounts

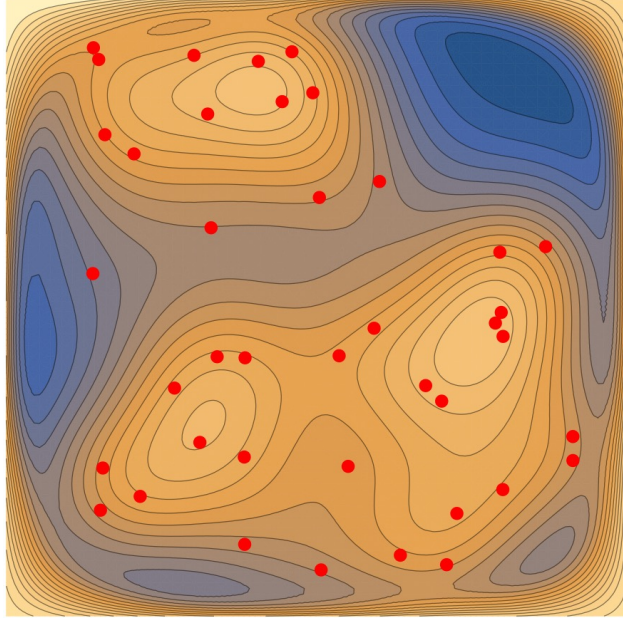


**Figure 3.2.** Equipotentials in a typical disordered material. The red dots show random potential centers used to simulate this example. These equipotentials are localized and closed in the bulk while those at the boundary run along the entire perimeter of the material. Since guiding center eigenstates run along these equipotentials (see accompanying text), those in the bulk are localized. The extended guiding center states along the edge are the well-known edge states, which account for the quantized Hall conductance of a filled Landau level.

for the existence of plateaus in the QHE since the filling up of the bulk localized states does not change macroscopic transport coefficients. The quantized value of Hall conductance can then be derived using standard techniques [17] when the externally applied chemical potentials at the boundaries differentially populate edge states belonging to the same set of Landau levels.

### 3.2.2 Beyond Landau-level projection - an effective Hamiltonian

Next we take into account the second and higher order terms in Eq. (3.15). These account for the cyclotron motion induced ‘jitter’ in the electron’s position. Since we have assumed that  $V(\mathbf{r})$  varies slowly, we can look upon the higher order terms in Eq. (3.15) as location-dependent perturbations to the cyclotron orbits. To mathematically articulate this picture

we first fix the Landau level index,  $n$ , and the guiding center location,  $\mathbf{R}$ , and then find the new  $\mathbf{R}$ -dependent kinetic momentum eigenfunction using perturbation theory. Thus, the corrections take the form of a gradient expansion in the electric field; for the purposes of connecting to the gravitational response of quantum Hall states, we need to keep only the first few terms in Eq. (3.15).

Since we are mainly interested in response functions, we only need calculate the first two moments of GIV operators. To this end we will use the following trick to compactly organize the perturbation expansion. Consider a quantum harmonic oscillator Hamiltonian perturbed by operators that are symmetrized polynomials of the canonical pair of momentum and coordinate operators,  $(p, q)$ . We keep perturbations till the third degree:

$$\mathcal{H}_{\text{HO}} = \frac{p^2 + q^2}{2} + \epsilon \sum_{k=0}^3 S_k, \quad (3.20)$$

where  $S_k$  is a real polynomial of degree  $k$  in  $p$  and  $q$ , and all terms that mix  $p$  and  $q$  are symmetrized. For example, the general form of  $S_3$  is:

$$S_3 = ap^3 + b(p^2q + pqp + qp^2) + c(q^2p + qpq + pq^2) + dq^3,$$

where  $(a, b, c, d)$  are real numbers. Consider, for a given SHO level index  $n$ , an effective quadratic Hamiltonian,  $\mathcal{H}_{\text{HO}}^{(n)}$ , obtained by Wick-contracting each monomial to terms that are either degree 1 or 2 (i.e., linear or quadratic) in  $q$  and  $p$ ; each contraction is replaced by the expectation value in the unperturbed energy level with index  $n$ . For example, following this procedure,  $p^3 \rightarrow 3 \langle p^2 \rangle_n p = 3\chi_n p$ , where

$$\chi_n = n + \frac{1}{2} \quad (3.21)$$

is the expectation value of  $p^2$  (or  $q^2$ ) in the  $(n+1)^{\text{st}}$  energy eigenstate of the unperturbed SHO. Clearly, only  $S_3$  is modified by this procedure.

The utility of this procedure is that the expectation values of all observables which are linear or quadratic in  $q$  and  $p$ , in the perturbed eigenstate of Eq. (3.20) with index  $n$ ,

are obtained correctly to all orders in  $S_0, S_1$  and  $S_2$ , and only to linear order in  $S_3$ , when calculated using the  $(n+1)^{\text{st}}$  eigenstate of the effective Hamiltonian,  $\mathcal{H}_{\text{HO}}^{(n)}$ . That this is true can be checked by straightforward computation.

This key insight allows us to write down the following effective quadratic Hamiltonian for calculating properties of the  $(n+1)^{\text{st}}$  eigenstate of Eq. (3.12), using the gradient expansion in Eq. (3.15) and keeping up to the third order in derivatives of  $V$ :

$$\begin{aligned}\mathcal{H}^{(n)} = & \frac{\pi_a \pi_a}{2} - V(\mathbf{R}) - (\partial_a V(\mathbf{R})) (\epsilon_{ap} \pi_p) \\ & - \frac{1}{2} (\partial_{ab}^2 V(\mathbf{R})) (\epsilon_{ap} \epsilon_{bq} \pi_p \pi_q) - \\ & \frac{1}{2} (\partial_{abc}^3 V(\mathbf{R})) (\epsilon_{ap} \epsilon_{bq} \epsilon_{cr} \chi_n \delta_{pq} \pi_r). \end{aligned} \quad (3.22)$$

We have continued to use the Einstein summation convention for repeated indices, and also exploited the commutative property of partial derivatives. Using the identity  $\epsilon_{ap} \epsilon_{bq} = \delta_{ab} \delta_{pq} - \delta_{aq} \delta_{pb}$ , and substituting  $\mathbf{E} = -\nabla V$ ,

$$\begin{aligned}\mathcal{H}^{(n)} = & \frac{\pi_a \pi_a}{2} - V(\mathbf{R}) \\ & + \left[ E_a(\mathbf{R}) + \frac{\chi_n}{2} \partial_a (\nabla \cdot \mathbf{E}(\mathbf{R})) \right] (\epsilon_{ap} \pi_p) \\ & + \frac{1}{2} [(\nabla \cdot \mathbf{E}(\mathbf{R})) \delta_{ab} - \partial_a E_b(\mathbf{R})] \pi_a \pi_b. \end{aligned} \quad (3.23)$$

Note that we have used 2D divergence operators. Consequently, Gauss' law cannot be applied to replace  $\nabla \cdot \mathbf{E}$  with the charge density. Ignoring corrections that are nonlinear in the electric field, the effective Hamiltonian can be compactly expressed as

$$\mathcal{H}^{(n)} = \frac{g_{ab} (\pi_a - \Delta_a) (\pi_b - \Delta_b)}{2} - V(\mathbf{R}). \quad (3.24)$$

In the preceding expression, the new position-dependent ‘metric’ and divergence-free ‘drift’ corrections are, up to third (linear) order in the derivatives of  $V$ ,

$$g_{ab}(\mathbf{R}) = \delta_{ab} (1 + \nabla \cdot \mathbf{E}(\mathbf{R})) - \partial_a E_b(\mathbf{R}), \quad (3.25a)$$

$$\Delta_a(\mathbf{R}) = \epsilon_{ab} \left[ E_b(\mathbf{R}) + \frac{\chi_n}{2} \partial_b (\nabla \cdot \mathbf{E}(\mathbf{R})) \right]. \quad (3.25b)$$

As we show below, the determinant of  $g$  is responsible for a local modulation in the cyclotron orbit energies, while the unimodular part shears the cyclotron orbit. Thus, we expect the unimodular metric,  $G = g/\sqrt{\det g}$ , to be the metric relevant for topological response of the quantum Hall state [38]. A Gaussian curvature field,  $K_G(\mathbf{R})$ , can be extracted from this unimodular metric using the Brioschi formula [46]:

$$K_G(\mathbf{R}) = -\frac{\nabla^2 (\nabla_{\mathbf{R}} \cdot \mathbf{E}(\mathbf{R}))}{4}. \quad (3.26)$$

We will return to this expression for the curvature in a subsequent section. We note here that an alternate line of reasoning suggests that since  $g_{ab}$  appears in the place of an inverse mass matrix, the choice for the spatial metric is the inverse of  $G$  used above. This inverse choice will change the sign of the curvature derived above, leaving its magnitude unchanged.

In the presence of a non-uniform electric field the metric is no longer proportional to identity. Instead, the cyclotron orbit is stretched and rotated in a location-dependent manner. To see this note that the metric can be decomposed thus:

$$g = \sqrt{\det(g)} (\Lambda^{-1})^T \Lambda^{-1}, \quad (3.27)$$

where  $\Lambda^{-1}$  is a real matrix with unit determinant and composed of a shear and rotations (see below). To the linear third order derivative of  $V$ ,

$$\sqrt{\det(g)}(\mathbf{R}) = 1 + \frac{\nabla \cdot \mathbf{E}(\mathbf{R})}{2}, \quad (3.28a)$$

$$\Lambda_{ab}(\mathbf{R}) = \left( 1 - \frac{\nabla \cdot \mathbf{E}(\mathbf{R})}{4} \right) \delta_{ab} + \frac{\partial_a E_b}{2}. \quad (3.28b)$$

Eq. (3.27) allows us to locally define a rotated and appropriately-rescaled pair of modified kinetic momentum operators:

$$\mathbf{\Pi} = \Lambda^{-1} (\boldsymbol{\pi} - \boldsymbol{\Delta}). \quad (3.29)$$

These operators satisfy the same commutation relations as the original kinetic momenta. The guiding center variables,  $\mathbf{R}$ , also need modification to ensure that they commute with the modified kinetic momenta:

$$X_a = R_a + (\partial_p \Delta_a) \pi_p - \frac{1}{2} \epsilon_{ar} \epsilon_{ps} (\partial_r \Lambda_{sq}) \pi_p \pi_q, \quad (3.30)$$

where  $\Delta$  and  $\Lambda$  are evaluated at  $\mathbf{R}$ . To third order in derivatives of  $V$ , these modified guiding center variables,  $\mathbf{X}$ , commute with the modified kinetic momenta,  $\mathbf{\Pi}$ , and satisfy the GIV commutation relations, Eq. (3.1).

In terms of these modified GIVs, the effective quadratic Hamiltonian for calculating properties of the  $(n+1)^{\text{st}}$  eigenstate of Eq. (3.12) becomes that of a simple harmonic oscillator with a position-dependent cyclotron frequency:

$$\mathcal{H}^{(n)} = \omega(\mathbf{X}) \frac{\mathbf{\Pi}^2}{2} - V(\mathbf{X}), \quad (3.31)$$

where

$$\omega(\mathbf{X}) = \sqrt{\det(g(\mathbf{X}))} = 1 + \frac{\boldsymbol{\nabla} \cdot \mathbf{E}(\mathbf{X})}{2}. \quad (3.32)$$

To summarize, the  $(n+1)^{\text{st}}$  eigenstate of this Hamiltonian yields the correct linear and quadratic kinetic momentum operator moments, up to linear order in the background potential and the third order in derivatives of  $V(\mathbf{R})$  for a fixed value of  $\mathbf{R}$ . The  $n$ -dependence of this Hamiltonian is hidden in the definitions of the locally-varying parameters and definitions of the altered GIVs. This approach automatically takes into account Landau level mixing



by the electric field. For example, the local energy of a particle in the  $(n+1)^{\text{st}}$  Landau level is:

$$\begin{aligned} E_n(\mathbf{R}) &= \langle \mathcal{H}^{(n)} \rangle_n = \omega(\mathbf{R}) \left( n + \frac{1}{2} \right) - V(\mathbf{R}) \\ &= \left( 1 + \frac{\nabla \cdot \mathbf{E}(\mathbf{R})}{2} \right) \left( n + \frac{1}{2} \right) - V(\mathbf{R}). \end{aligned} \quad (3.33)$$

The local Landau level spacing is thus modified by a non-uniform electric field. This observable effect takes into account Landau-level-mixing by the electric field and was predicted earlier in [47], [48].

Before proceeding to calculate the response of other observables to the non-uniform electric field, we use the effective Hamiltonian in Eq. (3.31) to derive a simple geometric picture for the effect of the electric field on the cyclotron orbits. (See Figure 3.1.) Clearly, the form of Eq. (3.31) implies that the modified cyclotron orbits are circular in  $\Pi$ -space. The  $\Pi$  coordinates were obtained from the original kinetic momenta via the linear transformation, Eq. (3.29), which is the combination of a shift by  $\Delta$  and a unimodular transformation,  $\Lambda^{-1}$ . The transformation  $\Lambda$  can be decomposed [49] as:

$$\Lambda = R(-\theta) \cdot \begin{pmatrix} \lambda & 0 \\ 0 & \lambda^{-1} \end{pmatrix} \cdot R(\theta), \quad (3.34)$$

where  $\theta$  is the angle by which the coordinate axes need to be rotated to ensure that  $\partial_x E_x - \partial_y E_y$  is maximized.  $\lambda = 1 + (\partial_x E_x - \partial_y E_y)_{\text{max}} / 2$ , where the derivatives are evaluated in the new orientation specified by  $\theta$ . Thus, the cyclotron orbits in real space are sheared, with the long axis aligned with the  $x$ -axis of the rotated coordinate frame in which  $\partial_x E_x - \partial_y E_y$  is maximum. The ratio of the two axes of the elliptical orbit is given by  $\lambda^2$ . There are two additional modifications to the field-free cyclotron orbits. First, an orbit at the original field-free location  $\mathbf{R}$  is translated by an amount  $\delta(\mathbf{R}) = \langle \mathbf{r} - \mathbf{R} \rangle = \hat{\mathbf{z}} \times \Delta(\mathbf{R})$ . Second, these orbits are no longer stationary and acquire a drift velocity  $\mathbf{v}_d = \langle \boldsymbol{\pi} \rangle = \Delta(\mathbf{R})$  which is perpendicular to the shift,  $\delta(\mathbf{R})$ . Figure 3.1 summarizes these changes in the geometry of cyclotron orbits, when placed in an external electric field.

### 3.3 Local observables in a non-uniform electric field

Now we consider how different observable quantities change when a non-uniform field is switched on. Using our geometric picture we can delineate these changes as arising due to (i) displacement and drift i.e., (due to  $\Delta$ ) and (ii) shearing of the orbits (due to an effective distorted real space metric, whose effect is encapsulated in the matrix  $\Lambda$ ).

These calculations are succinct using the Wigner pseudoprobability formalism [50]. The central idea is to replace the quantum wavefunction, which is a function of one coordinate from each independent canonically conjugate pair of variables, by the Wigner pseudoprobability distribution, which is defined over the entire canonical phase space.

$$W_{\Psi}(\mathbf{R}, \mathbf{p}) = \iint \frac{dR}{2\pi} \frac{d\pi}{2\pi} \Psi^*(R_x + R/2, \pi_y + \pi/2) \times \\ \Psi(R_x - R/2, \pi_y - \pi/2) e^{i(R_y R + \pi_x \pi)}. \quad (3.35)$$

This formalism provides a natural framework for calculations involving GIVs, since typical observables expressed using GIVs do not favor any particular component in the canonical pair of guiding center coordinates. Given an operator  $\hat{\mathcal{O}}(\mathbf{R}, \boldsymbol{\pi})$ , where the products of canonically conjugate variables have been symmetrized, the expectation value of  $\hat{\mathcal{O}}$  in state  $\Psi$  is found by simply integrating the product of the Wigner function and the *classical* function  $\mathcal{O}(\mathbf{R}, \boldsymbol{\pi})$  over the  $R_x - R_y - \pi_x - \pi_y$  phase space.

Within the scheme of Landau-level projection, the Wigner function corresponding to the product wavefunctions in (3.16) is also a product of Wigner functions in the guiding center and kinetic momenta phase spaces:

$$\Psi_{m,n}(R_x, \pi_y) = \psi_m(R_x) \eta_n(\pi_y) \\ \Leftrightarrow W_{m,n}(\mathbf{R}, \mathbf{p}) = \mathcal{W}_m(\mathbf{R}) w_n(\boldsymbol{\pi}).$$

Using the effective Hamiltonian, Eq. (3.31), we conclude that the energy eigenstates are still of the form (3.16), except that they are functions of the modified  $\mathbf{\Pi} - \mathbf{X}$  phase space coordinate pairs (which were defined in Eqs. (3.29) and (3.30)):

$$W_{m,n}(\mathbf{R}, \mathbf{p}) = \mathcal{W}_m(\mathbf{X}) w_n(\mathbf{\Pi}). \quad (3.36)$$

Since the bulk guiding center wavefunctions,  $\psi_m$ , form a complete basis, we also have the following completeness relation, correct to the third linear order in derivatives of  $V$ :

$$\sum_m \mathcal{W}_m(\mathbf{R}) = \frac{1}{2\pi} = \sum_m \mathcal{W}_m(\mathbf{X}). \quad (3.37)$$

### 3.3.1 Local current density - analytical approach

Following Eq. (3.13), we consider the local single particle charge current density at location  $\mathbf{x}$ ,

$$\hat{\mathbf{j}}(\mathbf{x}) = -\frac{1}{2} \{ \hat{\boldsymbol{\pi}}, \delta(\hat{\mathbf{r}} - \mathbf{x}) \}. \quad (3.38)$$

Carets denote operators and we have used the fact that for quadratic dispersion the velocity operator is simply the kinetic momentum.

Within a single filled Landau level with index  $n$ , the sum of the expectation values of this operator in all single-particle states yields the total local current density,  $\mathbf{j}^{(n)}(\mathbf{x})$ . In component notation

$$\begin{aligned} j_a^{(n)}(\mathbf{x}) &= - \sum_m \iint d^2X d^2\Pi W_{m,n}(\mathbf{X}, \mathbf{\Pi}) \pi_a \delta^2(\mathbf{r} - \mathbf{x}) \\ &= - \iint \frac{d^2X d^2\Pi}{2\pi} w_n(\mathbf{\Pi}) \pi_a \delta^2(\mathbf{r} - \mathbf{x}). \end{aligned} \quad (3.39)$$

The completeness relation, Eq. (3.37), was used to eliminate the guiding center Wigner function. In this expression,  $\boldsymbol{\pi}$  and  $\mathbf{r}$  are functions of  $\mathbf{X}$  and  $\boldsymbol{\Pi}$ , as defined in Eqs. (3.29) and (3.30). Substituting these expressions,

$$j_a^{(n)}(\mathbf{x}) = - \iint \frac{d^2 X d^2 \Pi}{2\pi} w_n(\boldsymbol{\Pi}) (\Lambda \boldsymbol{\Pi} + \boldsymbol{\Delta})_a \times \delta^2[\mathbf{r}(\boldsymbol{\Pi}, \mathbf{X}) - \mathbf{x}], \quad (3.40)$$

where

$$r_a(\boldsymbol{\Pi}, \mathbf{X}) = X_a + \epsilon_{ab} \Delta_b(\mathbf{X}) + [\epsilon_{ac} \Lambda_{cb}(\mathbf{X}) - \partial_b \Delta_a(\mathbf{X})] \Pi_b + \frac{1}{2} \epsilon_{ar} \epsilon_{ps} (\partial_r \Lambda_{sq}(\mathbf{X})) \Pi_p \Pi_q. \quad (3.41)$$

The delta function in Eq. (3.40) has a zero at  $\mathbf{X} = \tilde{\mathbf{X}}$ :

$$\tilde{X}_a(\mathbf{x}) = x_a - \epsilon_{ab} \Pi_b + \dots, \quad (3.42)$$

where the ellipsis denote terms which are of the same order of smallness as the electric field. Thus, for any function  $F$ ,

$$\iint d^2 X \delta^2(\mathbf{r} - \mathbf{x}) F(\mathbf{X}) = J^{-1}(\mathbf{x}) F(\tilde{\mathbf{X}}(\mathbf{x})),$$

where  $J(\mathbf{x})$  is the Jacobian arising from the delta function integral:

$$\begin{aligned} J(\mathbf{x}) &= \left| \det \left( \frac{\partial r_a}{\partial X_b} \right) \right|_{\mathbf{X}=\tilde{\mathbf{X}}(\mathbf{x})} \\ &= [\epsilon_{ac} \partial_a \Delta_c(\mathbf{X}) + \epsilon_{ac} \Pi_p \partial_a \Lambda_{cp}(\mathbf{X})]_{\mathbf{X}=\tilde{\mathbf{X}}(\mathbf{x})} \\ &= 1 + \epsilon_{ac} \partial_a \Delta_c(\mathbf{x}) - \left( \partial_{aa}^2 \Delta_p(\mathbf{x}) - \epsilon_{ac} \partial_a \Lambda_{cp}(\mathbf{x}) \right) \Pi_p + \\ &\quad \left( \frac{\epsilon_{ab} \epsilon_{cp} \epsilon_{dq}}{2} \partial_{acd}^3 \Delta_b - \epsilon_{ac} \epsilon_{bq} \partial_{ab}^2 \Lambda_{cp} \right) \Pi_p \Pi_q. \end{aligned} \quad (3.43)$$

The above expression is correct to third order in derivatives of  $\mathbf{E}$ . Next,

$$\begin{aligned}
j_a^{(n)}(\mathbf{x}) &= - \iint \frac{d^2\Pi}{2\pi} w_n(\Pi) (\Lambda(\tilde{\mathbf{X}}(\mathbf{x}))\Pi + \Delta(\tilde{\mathbf{X}}(\mathbf{x}))_a J^{-1}(\mathbf{x})) \\
&= -\frac{\Delta_a(\mathbf{x})}{2\pi} - \left( -\epsilon_{de} \partial_d \Lambda_{ac} + \frac{1}{2} \epsilon_{bc} \epsilon_{de} \partial_{bd}^2 \Delta_a \right) \frac{\langle \Pi_c \Pi_e \rangle_n}{2\pi} \\
&\quad + \left( \epsilon_{dc} \partial_d \Lambda_{cb} - \partial_{dd}^2 \Delta_b \right) \frac{\langle \Pi_a \Pi_b \rangle_n}{2\pi} \\
&= -\frac{\Delta_a(\mathbf{x})}{2\pi} - \frac{\chi_n}{2\pi} \left( \frac{3}{2} \partial_{dd}^2 \Delta_a - 2\epsilon_{dc} \partial_d \Lambda_{ac} \right). \tag{3.44}
\end{aligned}$$

The current density can be separated into two contributions. First, a contribution arising from the drift-displacement vector,  $\Delta$ :

$$\begin{aligned}
[\mathbf{j}_\Delta^{(n)}(\mathbf{x})]_a &= -\frac{\Delta_a(\mathbf{x})}{2\pi} - \frac{3}{2} \partial_{dd}^2 \Delta_a \frac{\chi_n}{2\pi} \\
&= -\frac{\epsilon_{ab}}{2\pi} [\mathbf{E} + 2\chi_n \nabla (\nabla \cdot \mathbf{E})]_b. \tag{3.45}
\end{aligned}$$

Second, another contribution involving the shear matrix,  $\Lambda$ :

$$[\mathbf{j}_\Lambda^{(n)}(\mathbf{x})]_a = 2\epsilon_{dc} \partial_d \Lambda_{ac}(\mathbf{x}) \frac{\chi_n}{2\pi} = \frac{\epsilon_{ab} \chi_n}{2\pi} \frac{1}{2} [\nabla (\nabla \cdot \mathbf{E})]_b. \tag{3.46}$$

Adding these, we obtain the total current density contributed by a filled Landau level with index  $n$ :

$$\begin{aligned}
j_a^{(n)}(\mathbf{x}) &= [\mathbf{j}_\Delta^{(n)}(\mathbf{x})]_a + [\mathbf{j}_\Lambda^{(n)}(\mathbf{x})]_a \\
&= -\frac{\epsilon_{ab}}{2\pi} \left[ \mathbf{E} + \frac{3\chi_n}{2} \nabla (\nabla \cdot \mathbf{E}) \right]_b. \tag{3.47}
\end{aligned}$$

The preceding expression for linear response is correct up to the third order in derivatives of the electrostatic potential and agrees with previous derivations [43], [51].

It is known from field theoretical approaches [41], [43] that the coefficient of the second term in Eq. (3.47) arises from a combination of Hall viscosity and a term that originates from the swirling motion of cyclotron orbits [43]. Since the motion of cyclotron orbits is given by

the drift velocity,  $\mathbf{v}_d = \mathbf{\Delta}$ , which involves only  $\mathbf{\Delta}$ . We formulate the following conjecture: the Hall viscosity contribution (which is related to the gravitational coupling constant of quantum Hall states [38], [41], [43]) is given by  $\mathbf{j}_\Lambda^{(n)}(\mathbf{x})$ , the current density arising from the shearing of cyclotron orbits. The magnitude of  $\mathbf{j}_\Lambda^{(n)}(\mathbf{x})$  matches that obtained from the Hall viscosity contribution, thus yielding the correct values for the Hall viscosity and gravitational response coefficients.

### 3.3.2 Local charge density - analytical approach

Following Eq. (3.13), the single particle charge density operator at location  $\mathbf{x}$  is

$$\hat{\rho}(\mathbf{x}) = -\delta(\hat{\mathbf{r}} - \mathbf{x}). \quad (3.48)$$

Within a single filled Landau level with index  $n$ , the sum of the expectation values of this operator in all single-particle states yields the total local charge density,  $\rho^{(n)}(\mathbf{x})$ . Using techniques introduced previously for calculating the current density operator, we find:

$$\begin{aligned} \rho^{(n)}(\mathbf{x}) &= -\sum_m \iint d^2X d^2\Pi W_{m,n}(\mathbf{X}, \mathbf{\Pi}) \delta^2(\mathbf{r} - \mathbf{x}) \\ &= -\iint \frac{d^2X d^2\Pi}{2\pi} w_n(\mathbf{\Pi}) \delta^2(\mathbf{r} - \mathbf{x}) \\ &= -\iint \frac{d^2\Pi}{2\pi} w_n(\mathbf{\Pi}) J^{-1}(\mathbf{x}) \\ &= -\frac{1}{2\pi} \left[ 1 - \epsilon_{ac} \partial_a \Delta_c(\mathbf{x}) - \right. \\ &\quad \left. \chi_n \left( \frac{\nabla^2 (\epsilon_{ab} \partial_a \Delta_b)}{2} - \epsilon_{ac} \epsilon_{bp} \partial_{ab}^2 \Lambda_{cp} \right) \right]. \end{aligned} \quad (3.49)$$

The expression above is correct to third order in derivatives of the electric field. Using  $\rho_0 = -(2\pi)^{-1}$  to denote charge density in the absence of electric field, the contributions from  $\Delta$  and  $\Lambda$  can be separated as follows:

$$\begin{aligned} \left[ \frac{\rho^{(n)}(\mathbf{x}) - \rho_0}{\rho_0} \right]_{\Delta} &= -\epsilon_{ac} \partial_a \Delta_c(\mathbf{x}) - \frac{\chi_n}{2} \nabla^2 (\epsilon_{ab} \partial_a \Delta_b) \\ &= \nabla \cdot \mathbf{E}(\mathbf{x}) + \chi_n \nabla^2 (\nabla \cdot \mathbf{E}) + \dots \end{aligned} \quad (3.50a)$$

$$\begin{aligned} \left[ \frac{\rho^{(n)}(\mathbf{x}) - \rho_0}{\rho_0} \right]_{\Lambda} &= \chi_n \epsilon_{ac} \epsilon_{bp} \partial_{ab}^2 \Lambda_{cp} \\ &= -\frac{\chi_n}{4} \nabla^2 (\nabla \cdot \mathbf{E}) + \dots \end{aligned} \quad (3.50b)$$

Adding these contributions, the local fractional change in charge density becomes:

$$\frac{\rho^{(n)}(\mathbf{x}) - \rho_0}{\rho_0} = \nabla \cdot \mathbf{E}(\mathbf{x}) + \frac{3\chi_n}{4} \nabla^2 (\nabla \cdot \mathbf{E}) + \dots \quad (3.51)$$

Our result is consistent with previous calculations on the linear response of quantum Hall states [51], [52].

The contribution (Eq. (3.50a)) from the orbital shift field,  $\Delta$ , can be interpreted simply in terms of the geometric picture sketched in Figure 3.1. The non-uniform electric field causes the orbit at location  $\mathbf{X}$  to shift by an amount  $\delta(\mathbf{X}) = \hat{\mathbf{z}} \times \Delta(\mathbf{X})$ . Ignoring the effects of orbit shear, this induces a coarse-grained charge polarization field  $\mathbf{P}(\mathbf{X}) = \rho_0 \delta(\mathbf{X})$ . This polarization field induces an excess charge  $\rho(\mathbf{x}) - \rho_0 = -\langle \nabla \cdot \mathbf{P}(\tilde{\mathbf{X}}(\mathbf{x})) \rangle$ , a standard result in the study of electrostatics in continuous media; the angular brackets denote an average over orbits which contribute to the charge at  $\mathbf{x}$  while  $\tilde{\mathbf{X}}(\mathbf{x})$  was defined in Eq. (3.42). Expressing  $\mathbf{P}$  in terms of  $\Delta$  and using Eq. (3.42), we arrive at the  $\Delta$ -contributions in Eqs. (3.50a) and (3.51).

We can obtain the contribution (Eq. (3.50b)) from the shearing field,  $\Lambda$ , by exploiting an apparently unrelated property of quantum Hall states. It is known that spatial curva-

ture induces excess charge in quantum Hall states [38], a phenomenon we term topological gravitational response. For the fully filled Landau level with index  $n$ , this becomes:

$$\delta\rho_G(\mathbf{x}) = -\frac{\kappa}{2\pi}K_G(\mathbf{x}) \equiv \rho_0\chi_n K_G(\mathbf{x}), \quad (3.52)$$

where  $K_G(\mathbf{x})$  is the local Gaussian curvature and  $\delta\rho_G$  denotes the change in charge density arising due to topological gravitational response.  $\chi_n$  is the value of the gravitational coupling constant,  $\kappa$ , associated with a fully-filled Landau level with index  $n$ .  $\kappa$  is believed to be a topologically-protected quantity which can only take up rational fraction values.

While there is no literal real-space curvature in the scenario we are considering, we have already noted that the non-uniform electric field can induce a fictitious Gaussian curvature, given by Eq. (3.26). Therefor, we conjecture that the introduction of this curvature has the same effect as that of a spatial curvature with the same magnitude. Then it follows that the physics of topological gravitational response contributes the following amount to the induced charge:

$$\delta\rho_G(\mathbf{x}) = -\rho_0\frac{\chi_n}{4}\nabla^2(\nabla\cdot\mathbf{E}). \quad (3.53)$$

This is exactly the value obtained from the shear contribution, Eq. (3.50b). We have thus shown that topological gravitational response apparently contributes to the local charge density response of quantum Hall states in non-uniform electric fields.

We conclude this section with the following conjecture, in analogy with the connection between the current density response and the gravitational coupling constant [41], [43]. We expect that the charge density response to a non-uniform electric field should have the form:

$$\rho(\mathbf{x}) - \rho_0 = -\nabla\cdot\mathbf{P}(\mathbf{x}) + \frac{\kappa}{2\pi}\frac{\nabla^2(\nabla\cdot\mathbf{E})}{4} + \dots, \quad (3.54)$$

where  $\rho_0$  is the charge density in the absence of any electric field,  $\kappa$  is the gravitational coupling constant and  $\mathbf{P}(\mathbf{x})$  is the averaged polarization field caused by shifts in the guiding centers.



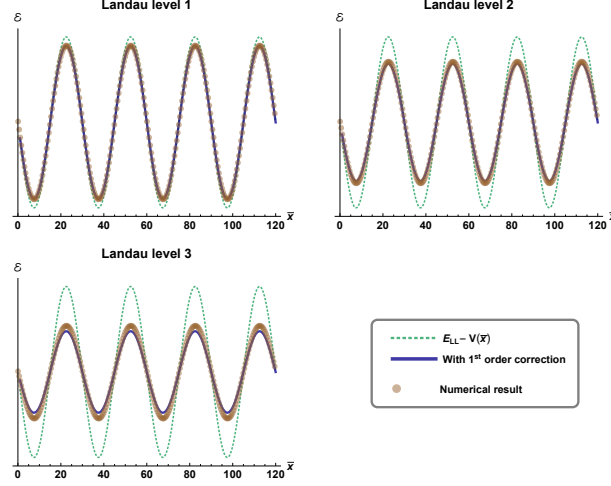


**Figure 3.3.** The variation of cyclotron orbit energy with orbit location,  $\bar{x}$ . The Landau levels are modeled by the lowest bands in a Hofstadter model on a square lattice. The nonuniform electric field is generated by a sinusoidal background potential, which is small compared to the inter-Landau-level energy gap, so that the system is in the linear response regime. The brown circles correspond to the cyclotron energies obtained via numerical diagonalization. The dashed green curve is the sum of the Landau level energy and the local potential energy, which is the correct energy when the electric field is uniform. The thick blue curve corresponds to Eqs. (3.33) and (3.55), correct up to the second order in the derivatives of the electric field. For these plots,  $V_0/\epsilon_c = 0.05$ ,  $k\ell = 0.65$ .

### 3.3.3 Numerical checks of analytical calculations

Now we provide numerical checks for our analytical results on how local observables change as a function of a spatially-varying electric field. To this end we construct a Hofstadter model on a square lattice with nearest-neighbor hopping and periodic boundary conditions in the  $x$ -direction. To this we add a sinusoidally-varying on-site electrostatic potential,  $V(x) = V_0 \sin kx$ . We use the Landau gauge,  $\mathbf{A} = Bx\hat{\mathbf{y}}$ , yielding eigenstates which are extended in the  $y$ -direction but localized in the  $x$ -direction. In this system, it is natural to set the hopping amplitude, the lattice spacing, Planck's constant,  $\hbar$ , and the magnitude of electronic charge,  $e$ , to unity. In these units, we choose the magnetic field to be  $B = 1/q$ , where  $q \gg 1$ . With this choice, the lowest few Landau levels have the same characteristics as obtained for a continuum model with quadratically-dispersing particles. Diagonalizing the

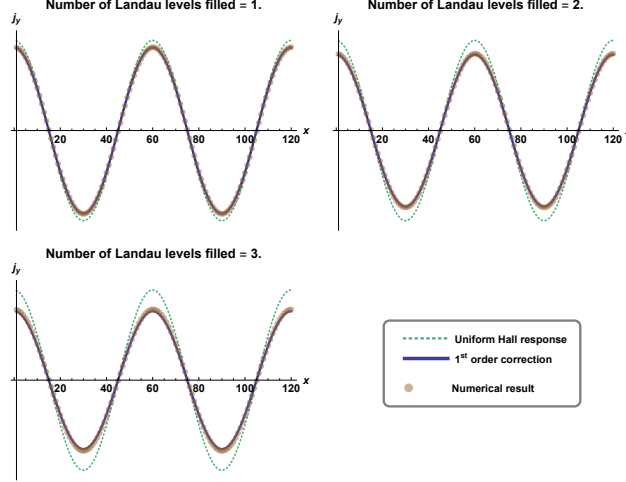


**Figure 3.4.** The spatial variation of local current density in a nonuniform (sinusoidal) electric field. The Landau levels are modeled by the lowest bands in a Hofstadter model on a square lattice. The nonuniform electric field is generated by a sinusoidal background potential, which is small compared to the inter-Landau-level energy gap so that the system is in the linear response regime. The brown circles correspond to the local current density values obtained via numerical diagonalization. The dashed green curve is the quantized local Hall response, which is correct when the electric field is uniform. The thick blue curve corresponds to Eqs. (3.47) and (3.56), correct up to the second order in the derivatives of the electric field. For these plots,  $V_0/\epsilon_c = 0.05$ ,  $k\ell = 0.32$ .

Hamiltonian, we obtain the spatial variation of cyclotron orbit energies, the local charge-current density and the charge density.

Below, we use slightly modified units better-suited for the Hofstadter model: the units of length and energy are respectively set to the lattice spacing and the nearest-neighbor hopping amplitude. In these units the magnetic length is  $\ell = \sqrt{q/2\pi}$  and the inter-Landau level (cyclotron) gap, in the continuum limit, is  $\epsilon_c = 4\pi/q$ . For  $k\ell \gg 1$  (slowly varying potential) and  $V_0 \ll \epsilon_c$  (weak potential) our results can be written as follows.

The cyclotron orbit energies (from Eq. (3.33)) become the local energy of each quantum state:

$$E_n(\bar{x}) = \left(n + \frac{1}{2}\right) - \left(1 - \frac{(k\ell)^2}{2} \left(n + \frac{1}{2}\right) + \dots\right) V_0 \sin k\bar{x}. \quad (3.55)$$

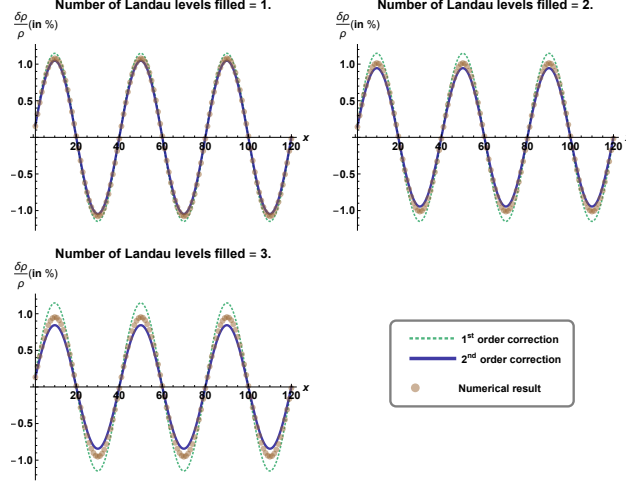


**Figure 3.5.** The spatial variation of local fractional charge density modulation in a nonuniform (sinusoidal) electric field. The Landau levels are modeled by the lowest bands in a Hofstadter model on a square lattice. The nonuniform electric field is generated by a sinusoidal background potential, which is small compared to the inter-Landau-level energy gap so that the system is in the linear response regime. The brown circles correspond to the local charge density values obtained via numerical diagonalization. The dashed green curve is the response obtained correct to the second derivative in the electric field, Eq. (3.50), corresponding to the nonuniform polarization induced by cyclotron orbit shifts. The thick blue curve corresponds to Eqs. (3.51) and (3.57), correct to the third order in the derivatives of the electric field. For these plots,  $V_0/\epsilon_c = 0.05$ ,  $k\ell = 0.49$ .

In this expression,  $\bar{x}$  denotes the average  $x$ -position of the quantum state and  $n$  denotes the index of the Landau level to which the orbit belongs. In Figure 3.3, we have shown the numerical verification for this relation for the lowest three Landau levels.

In the presence of a potential that varies only in the  $x$ -direction, only the  $y$ -component of the local current density is nonzero. Its value for a filled Landau level with index  $n$  is (using Eq. (3.47)):

$$j_y^{(n)}(\mathbf{x}) = kV_0 \cos kx \left( 1 - \frac{3(k\ell)^2}{2} \left( n + \frac{1}{2} \right) + \dots \right).$$

A convenient observable is the total current density when the first  $N$  Landau levels are completely filled. It is obtained by summing the preceding expression over  $n = 0, 1, \dots, N-1$ :

$$J_y^{(N)}(\mathbf{x}) = NkV_0 \cos kx \left( 1 - \frac{3N}{4}(k\ell)^2 + \dots \right). \quad (3.56)$$

We have used  $\sum_{n=0}^{N-1} \chi_n = N^2/2$ . The expression outside the brackets is the expected current profile for uniform Hall conductance. In Figure 3.4 we have shown the numerical verification of this result for the lowest three Landau levels.

Finally, our prediction (Eq. (3.51)) for the change in local charge density,  $\delta\rho^{(n)}(x) = \rho^{(n)}(x) - \rho_0$ , becomes:

$$\frac{\delta\rho^{(n)}(x)}{\rho_0} = (k\ell)^2 \left( 1 - \frac{3(k\ell)^2}{4} \left( n + \frac{1}{2} \right) + \dots \right) \frac{V_0 \sin kx}{\epsilon_c}.$$

We have used the field-free cyclotron gap,  $\epsilon_c = 4\pi/q$ , to scale quantities with dimensions of energy. The second term in the bracket corresponds to the fourth-order derivative of the potential. Previously, we provided a conjecture for the value of its coefficient by connecting it to the topological gravitational response of quantum Hall states: as expected, it is found to be half the gravitational coupling constant. Again, a convenient observable is the fractional change in the total charge density,  $\rho_{\text{tot}}^{(N)}(x)$ , when the first  $N$  Landau levels are full:

$$\frac{\delta\rho_{\text{tot}}^{(N)}(x)}{\rho_0} = (k\ell)^2 \left( 1 - \frac{3N}{8}(k\ell)^2 + \dots \right) \frac{V_0 \sin kx}{\epsilon_c}. \quad (3.57)$$

In Figure 3.5, we have shown the numerical verification of this relation for the lowest three Landau levels.

### 3.4 Summary

In this chapter we have included a background electrostatic potential, which gives rise to a non-uniform electric field, and ignored interactions. Using the GIV representation we have derived a geometric picture of the response of cyclotron orbits to a non-uniform electric field, as summarized in Fig. 3.1. To recapitulate, the orbits get sheared, are shifted from their

original position, and drift in a direction perpendicular to the shift. These modifications are characterized by an effective shearing metric,  $g$ , and a vector field,  $\Delta$ , which controls both orbit drift and location shift;  $g$  and  $\Delta$  are defined in Eqs. (3.25a) and (3.25b), respectively.

We have combined this geometric picture and the Wigner quasiprobability formalism to calculate the linear local responses to the nonuniform electric field, as gradient expansions to the second order in derivatives of the electric field. Specifically, we calculated the local cyclotron orbit energy (Eq. (3.33)), the local current density (Eq. (3.47)), and the local charge density (Eq. (3.51)).

These calculations provide mechanistic insights as to why the gravitational coupling constant (defined as  $\kappa$  in Eq. (3.52)) appears in the current response to a nonuniform electric field [41], [43]. Motivated by our calculation of the local current density response, we were led to the conjecture that the current contribution from the shearing of the cyclotron orbit is the same as the previously-obtained current contribution involving the gravitational coupling constant [43]. Following this, we pursued a stronger conjecture – that the metric induced by non-uniform electric fields acts upon the quantum Hall state in the same way as a bona fide real-space metric with a Gaussian curvature given by Eq. (3.26) – in the context of charge density response to a non-uniform electric field. We found that the gravitational coupling constant appears in the local charge density response and enters the electric field gradient expansion for charge response at the third order, Eq. (3.54).

## REFERENCES

- [1] K. v. Klitzing, G. Dorda, and M. Pepper, “New method for high-accuracy determination of the fine-structure constant based on quantized hall resistance,” *Phys. Rev. Lett.*, vol. 45, pp. 494–497, 6 Aug. 1980. DOI: [10.1103/PhysRevLett.45.494](https://link.aps.org/doi/10.1103/PhysRevLett.45.494). [Online]. Available: <https://link.aps.org/doi/10.1103/PhysRevLett.45.494>.
- [2] D. C. Tsui, H. L. Stormer, and A. C. Gossard, “Two-dimensional magnetotransport in the extreme quantum limit,” *Phys. Rev. Lett.*, vol. 48, pp. 1559–1562, 22 May 1982. DOI: [10.1103/PhysRevLett.48.1559](https://link.aps.org/doi/10.1103/PhysRevLett.48.1559). [Online]. Available: <https://link.aps.org/doi/10.1103/PhysRevLett.48.1559>.
- [3] R. B. Laughlin, “Anomalous quantum hall effect: An incompressible quantum fluid with fractionally charged excitations,” *Phys. Rev. Lett.*, vol. 50, pp. 1395–1398, 18 May 1983. DOI: [10.1103/PhysRevLett.50.1395](https://link.aps.org/doi/10.1103/PhysRevLett.50.1395). [Online]. Available: <https://link.aps.org/doi/10.1103/PhysRevLett.50.1395>.
- [4] B. I. Halperin and J. K. Jain, *Fractional Quantum Hall Effects: New Developments*. World Scientific, 2020.
- [5] R. B. Laughlin, “Quantized hall conductivity in two dimensions,” *Phys. Rev. B*, vol. 23, pp. 5632–5633, 10 May 1981. DOI: [10.1103/PhysRevB.23.5632](https://link.aps.org/doi/10.1103/PhysRevB.23.5632). [Online]. Available: <https://link.aps.org/doi/10.1103/PhysRevB.23.5632>.
- [6] R. B. Laughlin, “Nobel lecture: Fractional quantization,” *Rev. Mod. Phys.*, vol. 71, pp. 863–874, 4 Jul. 1999. DOI: [10.1103/RevModPhys.71.863](https://link.aps.org/doi/10.1103/RevModPhys.71.863). [Online]. Available: <https://link.aps.org/doi/10.1103/RevModPhys.71.863>.
- [7] Q. Niu, D. J. Thouless, and Y.-S. Wu, “Quantized hall conductance as a topological invariant,” *Phys. Rev. B*, vol. 31, pp. 3372–3377, 6 Mar. 1985. DOI: [10.1103/PhysRevB.31.3372](https://link.aps.org/doi/10.1103/PhysRevB.31.3372). [Online]. Available: <https://link.aps.org/doi/10.1103/PhysRevB.31.3372>.
- [8] M. H. Johnson and B. A. Lippmann, “Motion in a constant magnetic field,” *Phys. Rev.*, vol. 76, pp. 828–832, 6 Sep. 1949. DOI: [10.1103/PhysRev.76.828](https://link.aps.org/doi/10.1103/PhysRev.76.828). [Online]. Available: <https://link.aps.org/doi/10.1103/PhysRev.76.828>.
- [9] J. K. Jain, *Composite fermions*. Cambridge University Press, 2007.
- [10] E. C. G. Sudarshan, “Equivalence of semiclassical and quantum mechanical descriptions of statistical light beams,” *Phys. Rev. Lett.*, vol. 10, pp. 277–279, 7 Apr. 1963. DOI: [10.1103/PhysRevLett.10.277](https://link.aps.org/doi/10.1103/PhysRevLett.10.277). [Online]. Available: <https://link.aps.org/doi/10.1103/PhysRevLett.10.277>.

- [11] R. J. Glauber, “Coherent and incoherent states of the radiation field,” *Phys. Rev.*, vol. 131, pp. 2766–2788, 6 Sep. 1963. DOI: [10.1103/PhysRev.131.2766](https://doi.org/10.1103/PhysRev.131.2766). [Online]. Available: <https://link.aps.org/doi/10.1103/PhysRev.131.2766>.
- [12] R. J. Glauber, “The quantum theory of optical coherence,” *Phys. Rev.*, vol. 130, pp. 2529–2539, 6 Jun. 1963. DOI: [10.1103/PhysRev.130.2529](https://doi.org/10.1103/PhysRev.130.2529). [Online]. Available: <https://link.aps.org/doi/10.1103/PhysRev.130.2529>.
- [13] J. R. Klauder and E. C. G. Sudarshan, *Fundamentals of Quantum Optics*. Dover, 2006.
- [14] A. Perelomov, “Generalized coherent states and their applications,” 1986. DOI: [10.1007/978-3-642-61629-7](https://doi.org/10.1007/978-3-642-61629-7).
- [15] G. Moore and N. Read, “Nonabelions in the fractional quantum hall effect,” *Nuclear Physics B*, vol. 360, no. 2-3, pp. 362–396, 1991.
- [16] T. H. Hansson, M. Hermanns, S. H. Simon, and S. F. Viefers, “Quantum hall physics: Hierarchies and conformal field theory techniques,” *Rev. Mod. Phys.*, vol. 89, p. 025 005, 2 May 2017. DOI: [10.1103/RevModPhys.89.025005](https://doi.org/10.1103/RevModPhys.89.025005). [Online]. Available: <https://link.aps.org/doi/10.1103/RevModPhys.89.025005>.
- [17] D. Yoshioka, *The quantum Hall effect*. Springer Science & Business Media, 2002, vol. 133.
- [18] J. D. Jackson, “Classical electrodynamics,” *American Institute of Physics*, vol. 15, no. 11, pp. 62–62, 2009.
- [19] T. A. Loring and M. B. Hastings, “Disordered topological insulators via  $c^*$ -algebras,” *EPL (Europhysics Letters)*, vol. 92, no. 6, p. 67 004, 2011.
- [20] F. Duncan and M. Haldane, “The hierarchy of fractional states and numerical studies,” in *The quantum Hall effect*, Springer, 1990, pp. 303–352.
- [21] R. R. Biswas, “Semiclassical theory of viscosity in quantum hall states,” *arXiv preprint arXiv:1311.7149*, 2013.
- [22] Y. Chen, G. Jiang, and R. R. Biswas, “Geometric response of quantum hall states to electric fields,” *Phys. Rev. B*, vol. 103, p. 155 303, 15 Apr. 2021. DOI: [10.1103/PhysRevB.103.155303](https://doi.org/10.1103/PhysRevB.103.155303).
- [23] A. A. Koulakov, M. M. Fogler, and B. I. Shklovskii, “Charge density wave in two-dimensional electron liquid in weak magnetic field,” *Phys. Rev. Lett.*, vol. 76, pp. 499–502, 3 Jan. 1996. DOI: [10.1103/PhysRevLett.76.499](https://doi.org/10.1103/PhysRevLett.76.499). [Online]. Available: <https://link.aps.org/doi/10.1103/PhysRevLett.76.499>.

- [24] B. I. Halperin, “Theory of the quantized hall conductance,” *Helvetica Physica Acta*, vol. 56, no. 1-3, pp. 75–102, 1983.
- [25] M. O. Goerbig and N. Regnault, “Analysis of a SU(4) generalization of halperin’s wave function as an approach towards a SU(4) fractional quantum hall effect in graphene sheets,” *Phys. Rev. B*, vol. 75, p. 241 405, 24 Jun. 2007. DOI: [10.1103/PhysRevB.75.241405](https://doi.org/10.1103/PhysRevB.75.241405). [Online]. Available: <https://link.aps.org/doi/10.1103/PhysRevB.75.241405>.
- [26] E. J. Bergholtz and A. Karlhede, “Half-filled lowest landau level on a thin torus,” *Phys. Rev. Lett.*, vol. 94, p. 026 802, 2 Jan. 2005. DOI: [10.1103/PhysRevLett.94.026802](https://doi.org/10.1103/PhysRevLett.94.026802). [Online]. Available: <https://link.aps.org/doi/10.1103/PhysRevLett.94.026802>.
- [27] A. G. Abanov and P. B. Wiegmann, “Quantum hydrodynamics, the quantum benjamin-ono equation, and the calogero model,” *Phys. Rev. Lett.*, vol. 95, p. 076 402, 7 Aug. 2005. DOI: [10.1103/PhysRevLett.95.076402](https://doi.org/10.1103/PhysRevLett.95.076402). [Online]. Available: <https://link.aps.org/doi/10.1103/PhysRevLett.95.076402>.
- [28] M. Horsdal and J. M. Leinaas, “Explicit mapping between a two-dimensional quantum hall system and a one-dimensional luttinger liquid. i. luttinger parameters,” *Phys. Rev. B*, vol. 76, p. 195 321, 19 Nov. 2007. DOI: [10.1103/PhysRevB.76.195321](https://doi.org/10.1103/PhysRevB.76.195321). [Online]. Available: <https://link.aps.org/doi/10.1103/PhysRevB.76.195321>.
- [29] A. Cappelli, C. A. Trugenberger, and G. R. Zemba, “Infinite symmetry in the quantum hall effect,” *Nuclear Physics B*, vol. 396, no. 2-3, pp. 465–490, 1993.
- [30] “The quantum hall effect,” R. E. Prange and S. M. Girvin, Eds., 1990. DOI: <https://doi.org/10.1007/978-1-4612-3350-3>.
- [31] I. G. Macdonald, *Symmetric functions and Hall polynomials*. Oxford university press, 1998.
- [32] F. D. M. Haldane, “Geometrical description of the fractional quantum hall effect,” *Phys. Rev. Lett.*, vol. 107, p. 116 801, 11 Sep. 2011. DOI: [10.1103/PhysRevLett.107.116801](https://doi.org/10.1103/PhysRevLett.107.116801). [Online]. Available: <https://link.aps.org/doi/10.1103/PhysRevLett.107.116801>.
- [33] B. Yang, Z.-X. Hu, Z. Papi  , and F. D. M. Haldane, “Model wave functions for the collective modes and the magnetoroton theory of the fractional quantum hall effect,” *Phys. Rev. Lett.*, vol. 108, p. 256 807, 25 Jun. 2012. DOI: [10.1103/PhysRevLett.108.256807](https://doi.org/10.1103/PhysRevLett.108.256807). [Online]. Available: <https://link.aps.org/doi/10.1103/PhysRevLett.108.256807>.
- [34] X.-G. Wen, *Quantum field theory of many-body systems: from the origin of sound to an origin of light and electrons*. Oxford University Press on Demand, 2004.



- [35] M. P. Zaletel and R. S. K. Mong, “Exact matrix product states for quantum hall wave functions,” *Phys. Rev. B*, vol. 86, p. 245 305, 24 Dec. 2012. DOI: [10.1103/PhysRevB.86.245305](https://doi.org/10.1103/PhysRevB.86.245305). [Online]. Available: <https://link.aps.org/doi/10.1103/PhysRevB.86.245305>.
- [36] C. Day, “Quantum spin hall effect shows up in a quantum well insulator, just as predicted,” *Physics Today*, vol. 61, no. 1, p. 010 000, 2008.
- [37] X.-L. Qi and S.-C. Zhang, “The quantum spin hall effect and topological insulators,” *arXiv preprint arXiv:1001.1602*, 2010.
- [38] X. G. Wen and A. Zee, “Shift and spin vector: New topological quantum numbers for the hall fluids,” *Phys. Rev. Lett.*, vol. 69, pp. 953–956, 6 Aug. 1992. DOI: [10.1103/PhysRevLett.69.953](https://doi.org/10.1103/PhysRevLett.69.953). [Online]. Available: <https://link.aps.org/doi/10.1103/PhysRevLett.69.953>.
- [39] R. R. Biswas and D. T. Son, “Fractional charge and inter-landau–level states at points of singular curvature,” *Proceedings of the National Academy of Sciences*, vol. 113, no. 31, pp. 8636–8641, 2016.
- [40] S. Klevtsov and P. Wiegmann, “Geometric adiabatic transport in quantum hall states,” *Phys. Rev. Lett.*, vol. 115, p. 086 801, 8 Aug. 2015. DOI: [10.1103/PhysRevLett.115.086801](https://doi.org/10.1103/PhysRevLett.115.086801). [Online]. Available: <https://link.aps.org/doi/10.1103/PhysRevLett.115.086801>.
- [41] N. Read, “Non-abelian adiabatic statistics and hall viscosity in quantum hall states and  $p_x + ip_y$  paired superfluids,” *Phys. Rev. B*, vol. 79, p. 045 308, 4 Jan. 2009. DOI: [10.1103/PhysRevB.79.045308](https://doi.org/10.1103/PhysRevB.79.045308). [Online]. Available: <https://link.aps.org/doi/10.1103/PhysRevB.79.045308>.
- [42] J. E. Avron, R. Seiler, and P. G. Zograf, “Viscosity of quantum hall fluids,” *Phys. Rev. Lett.*, vol. 75, pp. 697–700, 4 Jul. 1995. DOI: [10.1103/PhysRevLett.75.697](https://doi.org/10.1103/PhysRevLett.75.697). [Online]. Available: <https://link.aps.org/doi/10.1103/PhysRevLett.75.697>.
- [43] C. Hoyos and D. T. Son, “Hall viscosity and electromagnetic response,” *Phys. Rev. Lett.*, vol. 108, p. 066 805, 6 Feb. 2012. DOI: [10.1103/PhysRevLett.108.066805](https://doi.org/10.1103/PhysRevLett.108.066805). [Online]. Available: <https://link.aps.org/doi/10.1103/PhysRevLett.108.066805>.
- [44] J. Von Neumann, *Mathematische grundlagen der quantenmechanik*. Springer-Verlag, 2013, vol. 38.
- [45] B. I. Halperin, “Quantized hall conductance, current-carrying edge states, and the existence of extended states in a two-dimensional disordered potential,” *Phys. Rev. B*, vol. 25, pp. 2185–2190, 4 Feb. 1982. DOI: [10.1103/PhysRevB.25.2185](https://doi.org/10.1103/PhysRevB.25.2185). [Online]. Available: <https://link.aps.org/doi/10.1103/PhysRevB.25.2185>.

- [46] A. Gray, E. Abbena, and S. Salamon, *Modern differential geometry of curves and surfaces with Mathematica®*. Chapman and Hall/CRC, 2017.
- [47] H. A. Fertig and B. I. Halperin, “Transmission coefficient of an electron through a saddle-point potential in a magnetic field,” *Phys. Rev. B*, vol. 36, pp. 7969–7976, 15 Nov. 1987. DOI: [10.1103/PhysRevB.36.7969](https://doi.org/10.1103/PhysRevB.36.7969). [Online]. Available: <https://link.aps.org/doi/10.1103/PhysRevB.36.7969>.
- [48] F. D. M. Haldane and K. Yang, “Landau level mixing and levitation of extended states in two dimensions,” *Phys. Rev. Lett.*, vol. 78, pp. 298–301, 2 Jan. 1997. DOI: [10.1103/PhysRevLett.78.298](https://doi.org/10.1103/PhysRevLett.78.298). [Online]. Available: <https://link.aps.org/doi/10.1103/PhysRevLett.78.298>.
- [49] M. A. de Gosson, “Symplectic methods in harmonic analysis and in mathematical physics,” 2011. DOI: <https://doi.org/10.1007/978-3-7643-9992-4>.
- [50] J. E. Moyal, “Quantum mechanics as a statistical theory,” *Mathematical Proceedings of the Cambridge Philosophical Society*, vol. 45, no. 1, pp. 99–124, 1949. DOI: [10.1017/S0305004100000487](https://doi.org/10.1017/S0305004100000487).
- [51] S. H. Simon and B. I. Halperin, “Finite-wave-vector electromagnetic response of fractional quantized hall states,” *Phys. Rev. B*, vol. 48, pp. 17 368–17 387, 23 Dec. 1993. DOI: [10.1103/PhysRevB.48.17368](https://doi.org/10.1103/PhysRevB.48.17368). [Online]. Available: <https://link.aps.org/doi/10.1103/PhysRevB.48.17368>.
- [52] A. G. Abanov and A. Gromov, “Electromagnetic and gravitational responses of two-dimensional noninteracting electrons in a background magnetic field,” *Phys. Rev. B*, vol. 90, p. 014 435, 1 Jul. 2014. DOI: [10.1103/PhysRevB.90.014435](https://doi.org/10.1103/PhysRevB.90.014435). [Online]. Available: <https://link.aps.org/doi/10.1103/PhysRevB.90.014435>.